The effect of targeting TNFR2 and EPAC2 on humanized transgenic Alzheimer's disease mouse models

Using immunohistochemical and behavioural analyses to map the effects of TNFR2 agonist STAR2 and EPAC2 agonist S220 on Alzheimer's disease pathology in chronic and acute mouse models

By BSc Julia de Lange, S4162323, Master Biology student at the University of Groningen (RUG)

Presented on Friday 24 June 2022, report delivered on Friday 1 July 2022

Alzheimer's disease (AD) is the most prevalent neurodegenerative disease known today, has no cure available, and accounts for 60-80% of all dementia cases with numbers increasing worldwide. Impaired memory retrieval is attributed to the main symptoms of early AD: amyloid-beta (Aβ) plaques and hyperphosphorylated neurofibrillary tau tangles (NFTs), which may be the result or the cause of neuroinflammation in the brain. In our study we investigated the effect of stimulating the neuroprotective properties of receptor 2 (TNFR2) from the proinflammatory cytokine tumour necrosis alpha (TNF-α) secreted by activated microglia, by injecting the TNFR2 agonist STAR2 in a TNFR2-specific AD J20 mouse model. As rescuing impaired memory retrieval is also an important aim in treating AD, we examined the effect of EPAC2 activation (a protein associated with memory retrieval) through injections of our cAMP analogue, S220, into chronic and acute AD mouse models. Behavioural and immunohistochemical analyses were performed on the different AD mouse models to score effect of treatment on cognitive performance and AD pathology. Results showed reduced escape latency in Morris water maze tests for both STAR2- and S220-treated (not significant) mice compared to their control group, indicating improved memory and learning upon treatment with either compound in behavioural tests. Immunohistochemical stainings showed significantly reduced Aβ plaque levels in hippocampus and cortex regions with STAR2 treatment. Our findings show that TNFR2 activation alleviated AD neuropathology, while activation of TNFR2 and EPAC2 improve memory and learning in AD mouse models. Future research is necessary in order to provide more significant results for EPAC2 activation, whereas current results of TNFR2 stimulation are significantly promising.

Introduction

Issue

Alzheimer's disease (AD) is the most well-known, well-studied and prevalent type of neurodegenerative disease (NDD) today (list of abbreviations in Appendix 1: List of abbreviations). This age-related disease is primarily known for its main symptom: dementia, of which AD accounts for 60-80% of all cases[1–3]. The process of memory formation located in the hippocampus, where the memory is first acquired, then consolidated and finally retrieved, is no longer working (optimally) in patients with dementia[4]. Memory retrieval is the action when a conditioned stimulus leads to the accession and expression of a memory trace[5]. With an increasing number of patients running into the millions worldwide, the disease has yet to be cured[1]. Current AD treatments can alleviate symptoms, but fail to provide a cure as its neuropathology is still not fully understood[6–8]. However, most of ADs pathological hallmarks are known and occur prior or simultaneous to the onset of memory deficits (Figure 1)[9]. The hallmarks, mainly being elevated glial cell levels, intracellular deposition of

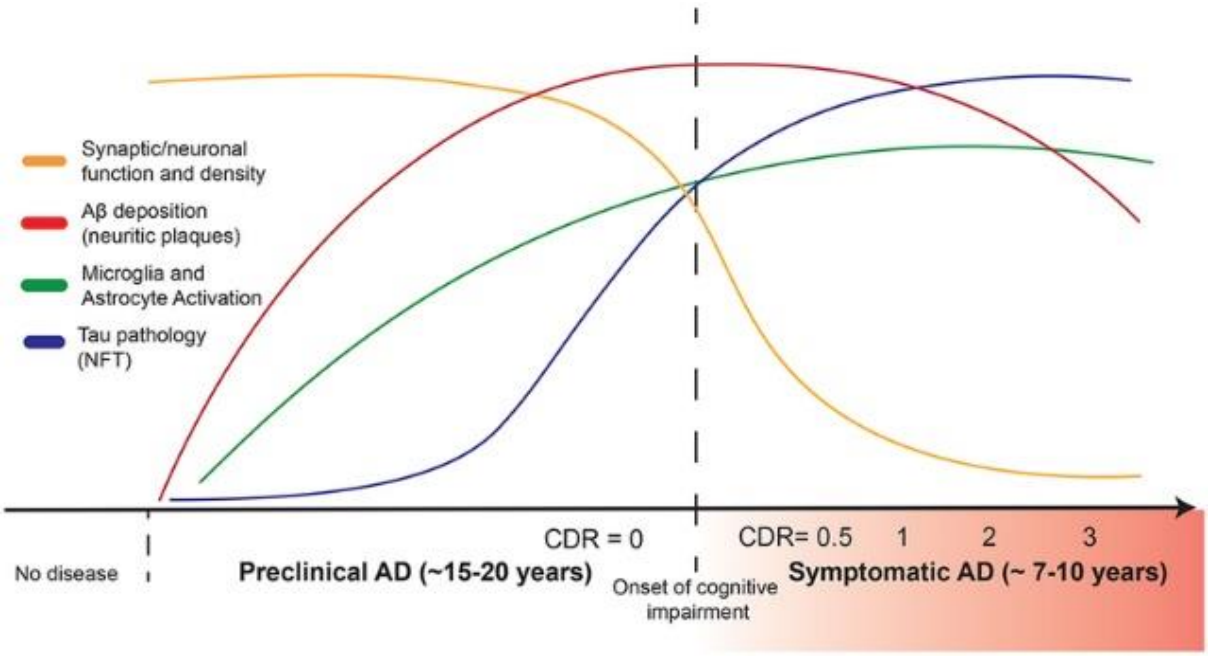

Figure 1 Onset and development of Alzheimer's disease's hallmarks, throughout the disease's progression. "Synaptic/neuronal function and density" resembles the 'quality of cognition'; "Microglia and Astrocyte Activation" indicates for glial cell activation; NFT = neurofibrillary tangle; CDR = clinical dementia rating (0: normal cognition, 0.5, 1, 2, and 3: questionable, mild, moderate, and severe dementia, respectively[9]. Source figure: [9].

hyperphosphorylated (neurofibrillary) tau tangles (NFT), and extracellular deposition of amyloid beta (Aβ) plaques in neurons, result in neuronal death in the hippocampus and are linked to memory deficits[1,10,11]. However, the correct order of occurrence of these hallmarks is still being debated[12]. NFTs are aggregates of tau, which is a microtubule-associated protein that maintains the structure of microtubules inside neurons, of which primarily axons. Microtubules are important in many vital cellular processes such as cell division, neurite differentiation and growth, as well as general neuronal activity. However, destabilized microtubules caused by tau aggregates, e.g. due to tau hyperphosphorylation, are linked to neurodegenerative diseases named tauopathies, among them is AD[13–15]. Aβ plaques are aggregates of said protein's oligomers[16–18]. Aβ is important for cognition, and necessary for synaptic plasticity and memory[19,20]. It is presumed to also play a role in tissue repair in the blood-brain barrier (BBB) and has functions in the immune system[20,21]. The Aβ protein is a product of cleavage of the amyloid precursor protein (APP) which can be cut in two different ways: via the non-amyloidogenic and the amyloidogenic pathway (Figure 2). In the non- amyloidogenic pathway, APP is cut by both γ-secretase and α-secretase, which leads to a variety of products, not associated to AD. The amyloidogenic pathway, however, is distinct for APP being cut by γ-secretase and β-secretase, resulting in the Aβ protein i.a.[22]. Both secretases can cleave Aβ on two different sites leading to a variety of possible Aβ types. However, the $Aβ_{40}$ and $Aβ_{42}$ variant of Aβ are most abundant in its plaques. $Aβ_{42}$ is considered the more insoluble form of Aβ, aggregates more easily, and in so doing aggravates the disease more strongly[23].

Regardless of the true chronology of AD onset, its pathology leads to increasing cognitive impairment, starting from mild forgetfulness in the early AD stage, to the moderate, middle stage where patients suffer from more typical AD symptoms such as the inability to learn new things, personality changes and restlessness, to the late, severe stage where the disease eventually leads to patients losing many physical abilities, and require full-time care[1,6,24]. Though many theories on the aetiology of AD are present[25], the amyloid cascade hypothesis[26] and, to a lesser extent,

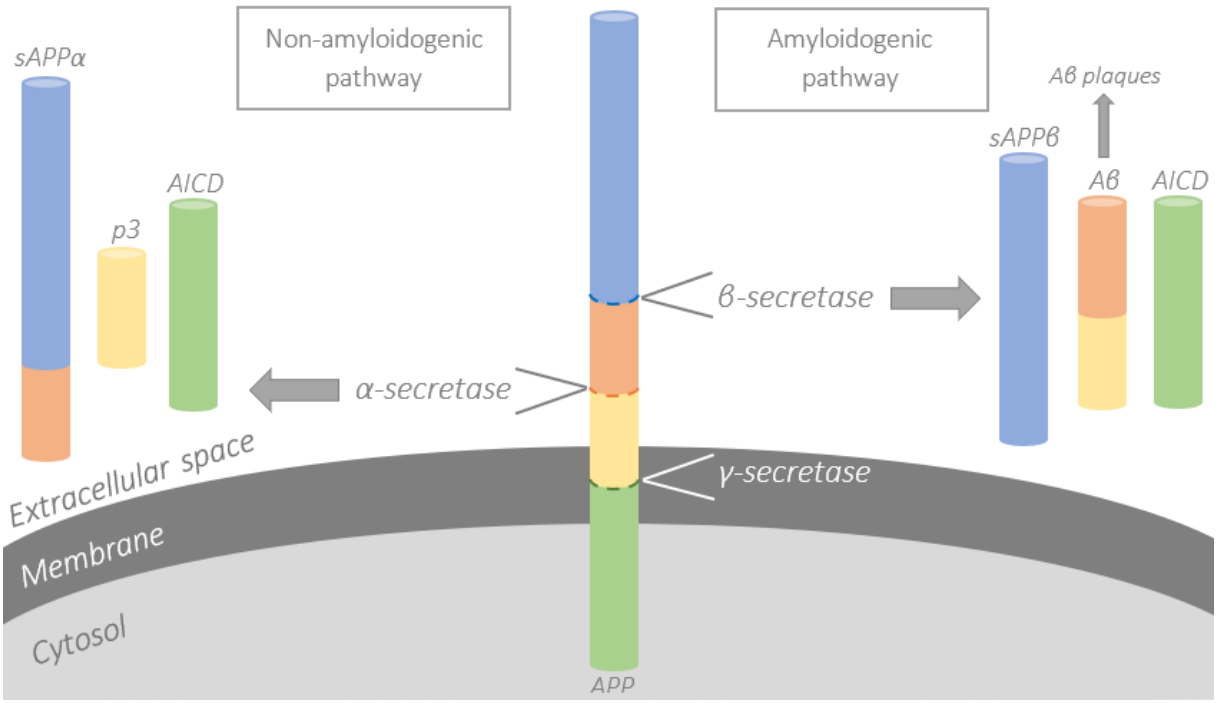

Figure 2 The amyloid precursor protein (APP) can undergo the non-amyloidogenic or the amyloidogenic pathway when cleaved by secretases. A- or β-secretase cuts first in the non-amyloidogenic pathway or amyloidogenic pathway, respectively. Γ-secretase cuts APP second in both pathways. Both β- and γ-secretase can cleave APP on two different sites, with the two most abundant types of Aβ in plaques being $Aβ_{40}$ and $Aβ_{42}$[23]. sAPP = soluble amino terminal ectodomain of APP; p3 = a short (protein) fragment; AICD = amyloid, or APP, intracellular domain; Aβ = amyloid beta, or beta-amyloid. Source figure: own figure.

the microglial dysfunction theory[27] are among the main approaches of many studies. The proposed chronology of AD hallmarks in these opposing theories are presented in Figure 3. In short, the microglial dysfunction theory states that the onset of AD is initially caused by aging which over time impairs microglial functions, leading to the degeneration of unsupported neurons, and hence the symptoms witnessed in AD[27]. The amyloid cascade hypothesis introduces the concept of incorrect cut Aβ protein, resulting in Aβ monomers aggregating into oligomers, which eventually leads to Aβ plaques that induce neuroinflammation. These plaques, as well as tau tangles, eventually cause neuron loss and lead in that way up to AD[27,28].

Although it remains unclear which theory is correct, the individual hallmarks (Figure 3) are in themselves good focus points for research and potential treatment for AD, as many studies have linked them to its pathogenesis. For example, neuroinflammation is a common hallmark witnessed in multiple other neurodegenerative diseases apart from AD, such as Parkinson's disease (PD) and amyotrophic lateral sclerosis (ALS)[29]. To better

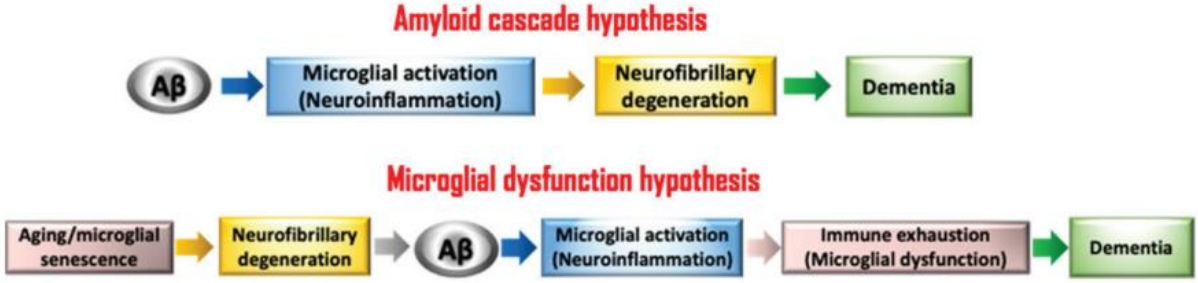

Figure 3 Amyloid cascade hypothesis and Microglial disfunction theory in relation to the onset of dementia, a symptoms witnessed in Alzheimer's disease. Aβ = amyloid beta. Source figure: [27].

understand the potential of intervening in the neuroinflammatory system, we need to look at its pathways. One cytokine involved in both inflammatory and neuroprotective responses is tumour necrosis factor alpha (TNF-α)[11,30]. Therefore, this master cytokine is the focus of part of this study.

Neuroinflammation and tumour necrosis factor-alpha

Together with chemokines and interleukins (IL-1β, IL-16, IL-18), TNF-α is excreted by activated microglia to activate other cells in order to deal with an immunological threat[29]. Various stimuli can trigger such an immunological response, such as pathogen- and damage-associated molecular patterns (PAMPs and DAMPs, respectively). Aβ is considered a (secondary) DAMP and is in so doing linked to TNF-α[31], by being able to trigger the release of this cytokine[32]. However, TNF-α induces Aβ production to begin with, turning these steps into a vicious circle that is hard to break[32]. As TNF-α activates microglia, overproduction of TNF-α can chronically activate the microglia due to this vicious circle. When AD progresses, proinflammatory cytokines, among them TNF-α, downregulate genes involved in the clearance of Aβ aggregates (e.g. the Aβ-degrading enzymes insulysin, and neprilysin, and Aβ scavenger receptor A) by microglia, making these cells dysfunctional and seemingly unable to clear the Aβ deposits in the presence of these inflammatory cytokines[33–35]. Therefore, we take a closer look at TNF-α for its potential in reducing Aβ production and Aβ related symptoms.

TNF-α is a type 2 transmembrane protein of 26 kDa that forms a stable homo-trimeric protein (tmTNF) that binds to both TNF receptor (TNFR) 1 and TNFR2. TmTNF can be cleaved by the TNF-α converting enzyme (TACE/ADAM17) to form the 17 kDa form of TNF which, in its homo-trimeric form of 51 kDa is known as the soluble form of TNF-α (solTNF) and binds mostly TNFR1 (Figure 4)[36]. TNF-α plays an important role in a variety of pathways, and has a pleiotropic function through TNFR1 and TNFR2, where it signals for neurodegeneration and inflammation, and neuroprotection, respectively[11].

TNF receptor 1

Binding of either solTNF (favoured) or tmTNF to TNFR1 leads to the activation of TNFR1's death domain (DD) which in turn interacts with TNF receptor 1 associated death domain (TRADD) protein (Figure 4). TRADD activates the assembly of proteins forming the TNFR1 signalling complex 1, which in turn can activate a variety of pathways. Among them the nuclear factor kappa-light-chain-enhancer of activated

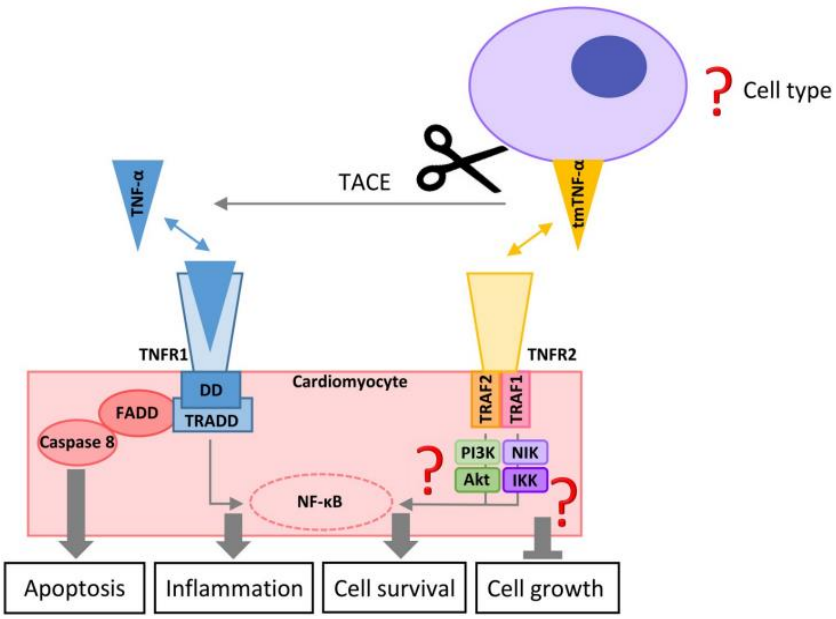

Figure 4 Tumour necrosis factor-alpha (TNF-α) is a pleiotropic, proinflammatory cytokine with two receptors (TNFR) where it activates pathways stimulating either neurodegeneration and inflammation (TNFR1) or neuroprotection (TNFR2). Transmembrane TNF-α (tm- TNF-α) binds mostly to TNFR2, and can be cleaved by TNF-α converting enzyme (TACE) into soluble TNF-α which binds mostly TNFR1. DD = death domain; TRADD = TNF receptor 1 associated death domain; FADD = Fas-associated protein with death domain; NF-κB = nuclear factor kappa-light-chain-enhancer of activated B cells; TRAF = TNF receptor-associated factor; PI3K = phosphatidyl inositol 3-kinase; NIK = NF-κB inducing kinase; Akt = protein kinase B; IKK = IκBα kinase. Source figure: [96]

B cells (NFκB) pathway, which can induce transcription of proinflammatory genes (e.g. for TNF-α, IL-6, and IL-8). This could in turn lead to a vicious circle of TNF-α activation, resulting in enhanced (neuro)inflammation. Apart from neuroinflammation, TNFR1 also causes apoptosis through formation of the pro-apoptotic signalling complex 2, which in turn induces apoptosis by the formation of the death-inducing signalling complex (DISC)[11,36,37].

TNF receptor 2

Though still not much is known about TNFR2, it is known that where activation of TNFR1 leads to cell death and inflammation, binding of (mostly) tmTNF to TNFR2 stimulates pathways that mediate mostly neuroprotection (Figure 4). Despite TNFR2 not having a DD and can therefore not directly induce cell death, it can activate the NFκB pathway indirectly through TNF receptor-associated factor (TRAF) 2 and induce neurodegeneration via that route, however this is an uncommon phenomenon[11,36].

TNFR2 agonist STAR2

As TNFR1 is expressed on virtually every different cell type in the body, TNFR2 is mostly confined to immune cells and endothelial cells[11]. Therefore, stimulating TNFR2 signalling in inflamed areas, such as the CNS in AD, might lead to cell survival and thus the rescue of neurons. Previous research showed the use of selective mouse TNF-based agonist of TNF receptor 2 (STAR2; Figure 5) in a study of graft-versus-host disease (GvHD), where regulatory T cells were expanded to protect patients from acute GvHD onset[38]. However, the use of STAR2 in AD pathology has yet to be examined elaborately, and brings about the potential of specific TNFR2 activation as a target for AD therapy[39]. The GvHD study showed STAR2 to be

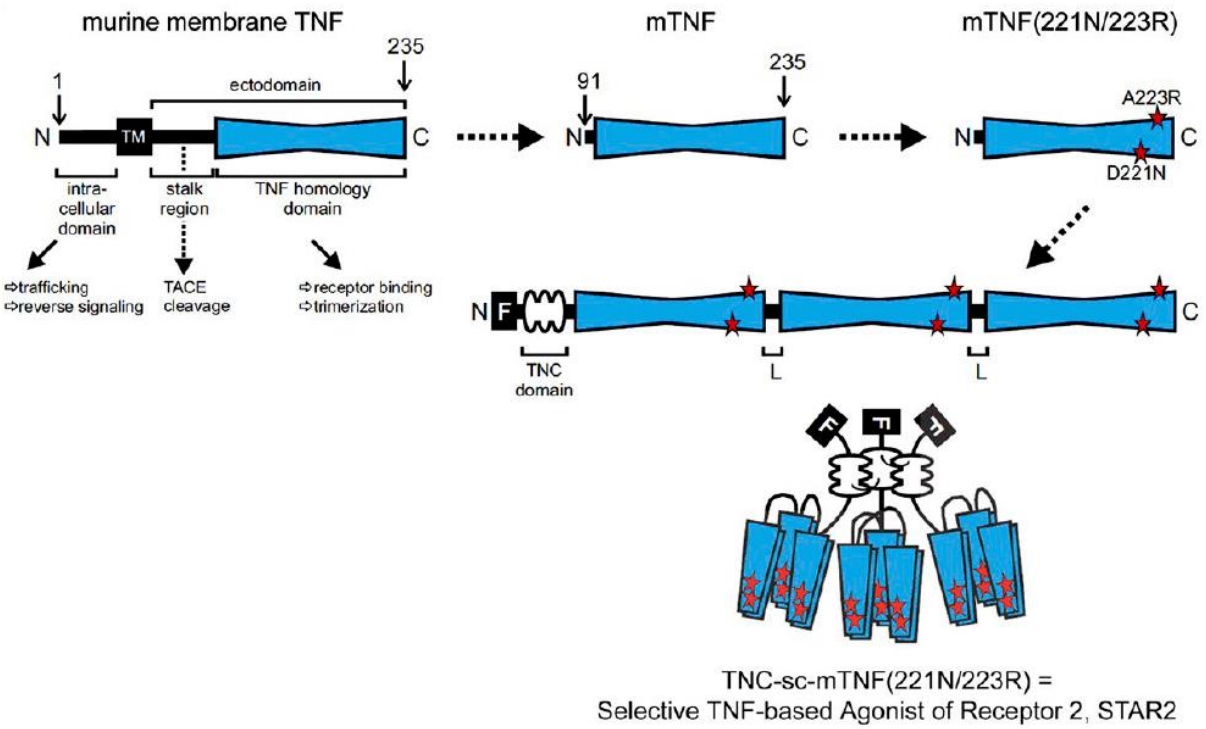

Figure 5 Assembly of selective TNF-based agonist of TNF receptor 2 (STAR2). Three linker-connected mTNF(221N/223R) promoters were adhered to the trimerization chicken tenascin-C (TNC)-domain, making three covalently linked TNF trimers that form the STAR2 molecule. F = Flag tag; L = linker; TACE = TNF-α converting enzyme; TM = transmembrane domain. Source figure: [38]

specific for TNFR2[38], rendering follow-up studies on its specificity as futile, and freeing the way to further research on its functionality in neurodegenerative diseases.

Ortí-Casañ et al. examined the effect of STAR2 on TNFR2 stimulation in an AD mouse model, where data showed reduced Aβ plaques and improvements in cognition (unpublished data). Our current study was partially a follow-up on this research and focused on the effect of STAR2 on neuroinflammation in the hippocampus compared to control group with phosphate-buffered saline (PBS) administration, as well as STAR2's effect on differences in memory through assessment of behavioural tests' results. Experiments testing STAR2's effectiveness have been performed on the same mouse species used in Ortí-Casañ et al.'s previous work, namely, J20 mice crossbred with human TNFR2 knock-in mice (kihuTNFR2). This kihuTNFR2 x J20 mouse model allows the pathology of AD to be displayed through the J20 part of the crossbreed by Aβ plaque formation (mainly in the hippocampus, but also in the neocortex)[40], synaptic loss, and cognitive impairment[41], and introduces the human TNFR2 receptor in this model through the kihuTNFR2 mice. In this study, only male mice have been used, in order to reduce the amount

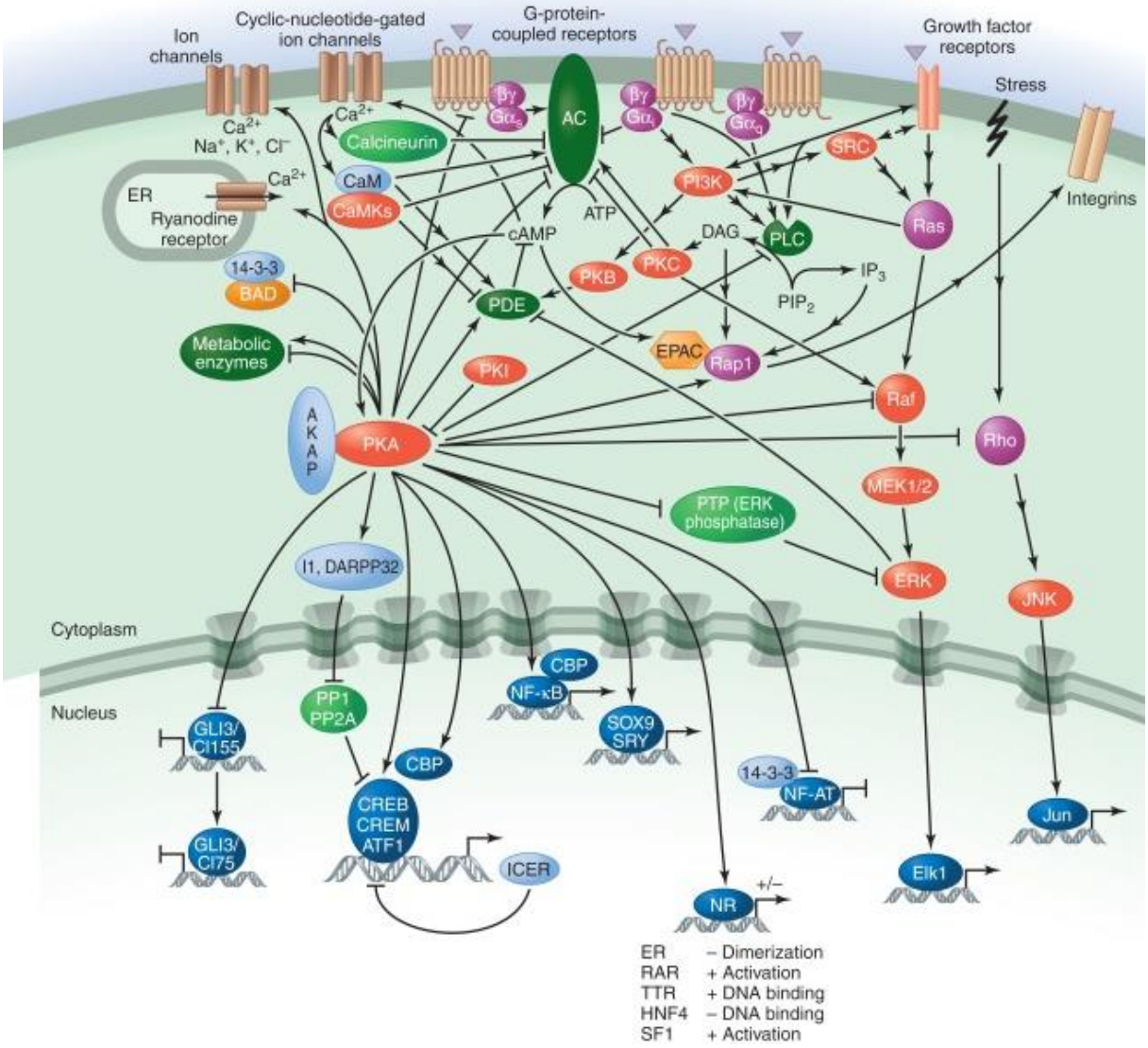

Figure 6 The cAMP/PKA pathway. Upon activation of a GPCR, downstream activation occurs via AC, which in turn activates cAMP. cAMP can activate both PKA and EPAC. GPCR: G-protein coupled receptor; AC: adenylyl cyclase; cAMP: cyclic adenosine monophosphate; PKA: protein kinase A; CREB: cAMP-response element-binding protein; NFκB: nuclear factor kappa B; EPAC: exchange protein directly activated by cAMP. For additional abbreviations, see source of the figure: [44].

of animals required and to eliminate influences of gender on study outcome. Memory was tested through behavioural experiments on a group of mice treated with the STAR2 compound and the control group, through the Morris water maze (MWM), elevated plus maze (EPM) and Y-maze experiments specifically to test spatial memory and learning, anxiety levels, and working memory, respectively. After behavioural experiments, mice were sacrificed and brain sections were used for investigating different aspects of AD neuropathology.

Memory (loss) and exchange protein activated by cyclic AMP (EPAC)

As mentioned earlier, TNF-α plays an important role in a variety of cascades. However, upstream of TNF-α is adenosine 3',5'-cyclic monophosphate, cyclic AMP, or simply cAMP, which is a secondary messenger molecule that plays a vital role in many pathways. cAMP is downstream of G-protein coupled receptors (GPCRs) and adenylyl cyclase (AC)[42], and can activate three main effectors, being cyclic-nucleotide-gated ion channels, protein kinase A (PKA) and exchange protein activated by cAMP (EPAC)[43,44] (Figure 6). PKA phosphorylates numerous metabolic enzymes, such as cAMP-response element-binding protein (CREB)[45], and is also involved in the NFκB pathway, which links back to TNF-α and its receptors[46]. EPAC is a less-studied protein that has two major isoforms, EPAC1 and EPAC2, encoded by the genes *Rapgef3* and *Rapgef4*, respectively[47]. EPAC proteins are guanine nucleotide exchange factors (GEFs) for Ras-like small GTPases, and are directly activated by cAMP (Figure 6), hence, synonyms for EPAC1 and EPAC2 are cAMP-GEF-1 and cAMP-GEF-2, respectively[48]. EPAC2 is a GEF for Rap1 and Rap2, which are Ras-like proteins. Rap1 and Rap2 are strictly regulated by GEFs and GTPase-activating proteins (GAPs), which they also should, as Rap functions are vital and therefore also more easily prone to detrimental consequences when not tightly regulated. Rap functions constitute of actin cytoskeleton-related regulation such as cell adhesion via integrin receptors, and specific cell junction formation[44,47], but also proliferation, apoptosis, exocytosis, migration, and carcinogenesis[49]. Rap1 can also trigger the extracellular-signal-regulated kinase (ERK) pathway[50].

Regarding the expression of the proteins, EPAC1 is mainly expressed ubiquitously in the body with low levels in the brain. Even though in a study with rats from Kawasaki et al. in 1998 EPAC1 was not expressed highly in adult brains, it was more prominent in neonatal brain areas, especially the septum and thalamus[51,52]. In contrast to EPAC1, EPAC2 is expressed primarily in the brain of both mature and neonatal rats, and in (neuro)endocrine tissues. In the brain EPAC2 plays a role in memory, learning, neurotransmitter release, neurite growth, neuronal differentiation, and in a few NDDs, among them AD[47,53]. Elevated messenger ribonucleic acid (mRNA) levels of EPAC2 found in the brain areas in this study were measured in the hippocampus (mostly in CA3 and the dentate gyrus), the cerebral cortex, the habenula, and the cerebellum[51]. Some studies have found the functions of both EPAC1 and EPAC2 to be opposing in other parts of the body than the brain, but also reported up-, and down-regulation of EPAC1 and EPAC2 mRNA levels in AD human brains, respectively[43]. Ostroveanu et al. investigated the effect of the EPAC activator 8-pCPT in mice, and found 8-pCPT to improve memory retrieval, but not memory acquisition nor memory consolidation[54]. Through this important function memory retrieval, henceforth, the focus of this second part of our study will be on EPAC2 and its relation to memory in AD pathology.

Memory retrieval and the AMPA receptor

As mentioned earlier, memory formation consists of three stages, them being acquisition, consolidation, and retrieval, the latter being impaired in AD[4]. When taking a look at the biological processes involved in memory, the α-amino-3-hydroxy-5-methyl-4-

isoxazolepropionic acid receptor (AMPAR)[55,56], an ionotropic glutamate receptor[57], is found to play an important role[55,56]. AMPAR blockage through the CNQX antagonist impaired memory retrieval in a study with rats[56], showing its necessity in memory retrieval function. AMPARs are often heteromeric tetramer receptors consisting of different subunit combinations, with the subunits being GluA1 to GluA4[55], though homomers have also been found[58]. The most common heteromer combinations for synaptic AMPARs are GluA1/2 and GluA2/3, accounting for 80% and 20% respectively in the CA1 region of the hippocampus[59]. AMPARs containing a GluA2 subunit show calcium impermeability (calcium impermeable AMPARs; CI-AMPARs), whereas AMPARs lacking this subunit show the opposite effect (calcium permeable AMPARS; CP-AMPARs) and play a unique role in synaptic activity[60]. Though, (CI-)AMPARs do aid indirectly in Ca^{2+} influx. Namely, when stimulated through binding of the neurotransmitter glutamate, AMPARs rapidly open up their channels which allows the influx of Na^{+} [60]. The sodium influx in turn causes depolarization in the neuron[60], which temporarily forces the Mg^{2+}-ion from its blocking position inside the channel of N-methyl-D-aspartate receptors (NMDARs), until the cell is repolarized again[61]. NDMARs are receptors important in neurotransmission[62] through providing Ca^{2+} current exchange and can only be efficient when its Mg^{2+}-ion is removed[61]. Hence, AMPARs and NMDARs work together to allow Ca^{2+} current to flow through the cell membrane to inside the cell in the postsynaptic terminal. This short influx is important in signal transduction as it stimulates downstream cascades, showing the NDMAR to be involved in synaptic transmission, plasticity, memory, and cognition[62,63].

Calcium influx through NMDARs also activates CREB and calmodulin-dependent kinase (CaMK) through phosphorylation, stimulates downstream gene transcription necessary for long-term potentiation (LTP), and regulates long-term depression (LTD)[62] (Figure 7). LTP is the strengthening process of synaptic transmission through activity-dependent plasticity[57]. It is also input-specific, lasts long[57], and is considered to be the molecular basis of neural plasticity and memory formation[62]. LTP expression is enhanced when an increase in AMPARs occurs. A decrease in the trafficking of AMPARs to the postsynaptic membrane is related to increased LTD expression[57]. Hence, through a loss of AMPARs at postsynaptic sites, LTD shows opposing effects of LTP. A study by Wong et al. showed LTD to impair memory retrieval due to acute stress[64], confirming LTP opposing effect. LTD of synaptic transmission has been found to be involved in AD memory impairment[65]. Prieto et al. found supporting evidence that AD-diseased synapses are intrinsically defective in LTP[66], implying for a likely need in arresting this defect and stimulating LTP in affected synapses in AD pathology.

LTP induction by NMDAR leads to recruitment of additional GluA1-containing AMPARs and possibly GluA2-containing AMPARs as well[67]. Trafficking of AMPARs is associated with LTP and LTD (Figure 7)[57]. After memory acquisition and consolidation, the abundance of GluA1/2 AMPARs are internalized, and replaced by GluA2/3 AMPARs, to enable and enhance memory retrieval[68]. Hence, in AD pathology Aβ inhibits NMDARs and presumably induces AMPAR downregulation, internalization and ubiquitination, which in turn restricts the receptors to execute their signal transduction function via limiting Ca^{2+} influx, and in so doing restrains memory and learning functions[61,69]. This makes stimulation of the GluA2/3 AMPAR, which has been linked to induce memory retrieval, a proper target to counter the loss of function in memory retrieval in AD[70]. EPAC2 also functions in long-term potentiation (LTP)[71] through interaction with glutamate receptor (GluA) 3[50], making our investigated cAMP analogue and EPAC2 activator Sp-8-BnT-cAMPS (S220) a promising compound for treatment.

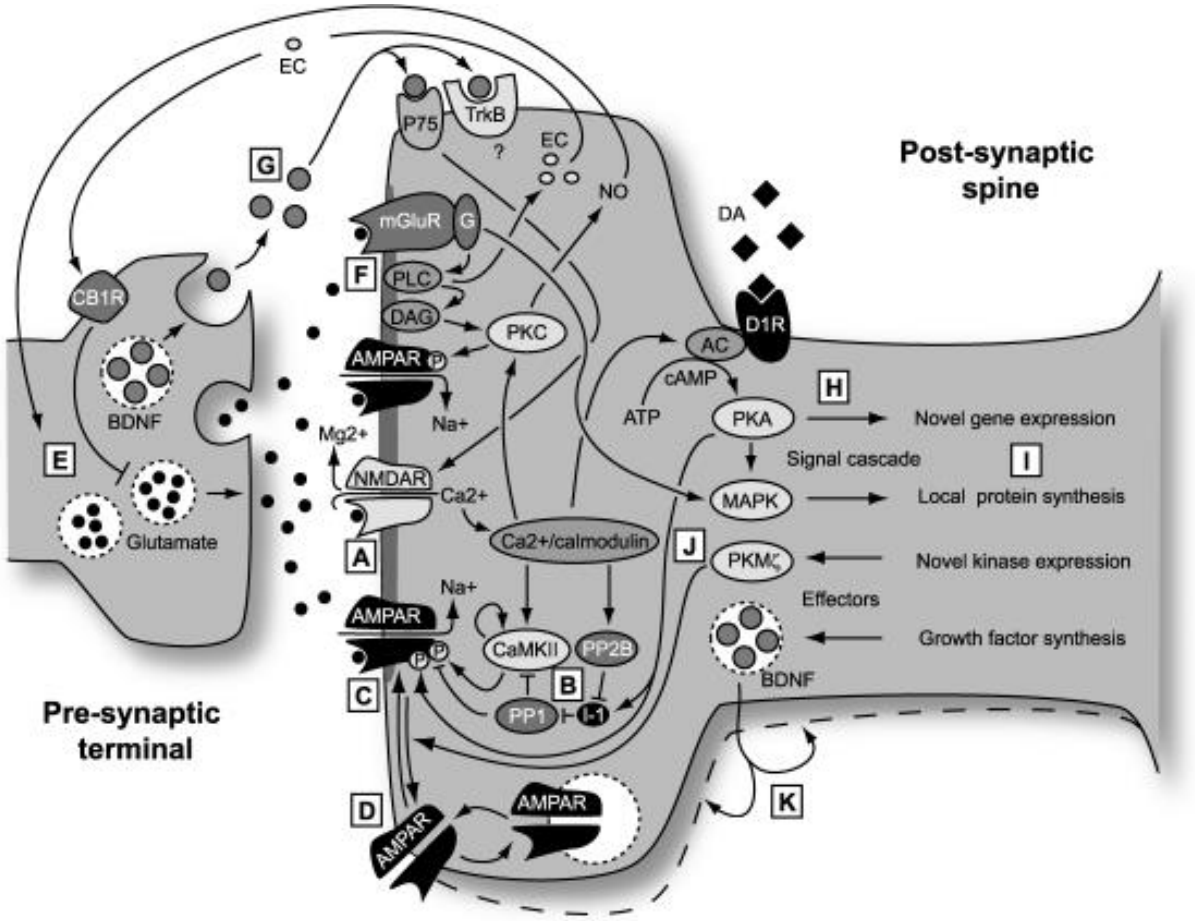

Figure 7 Long-term potentiation (LTP) and long-term depression (LTD) are activated through NMDAR activation (A).A concise summary from the figure source is given: B) Influx of calcium cations causes activation of downstream targets. C) LTP and LTD are expressed though phosphorylation and dephosphorylation of AMPARs, respectively. D) AMPAR trafficking influences LTP and LTD expression through increasing or decreasing its amount of receptors, respectively. E) NO and ECs can act as retrograde messengers signalling to the presynaptic cell that coincidence has occurred. F) Another form of LTD is dependent on group 1 mGluRs. G) BDNF contributes in different ways to both short- and long-term plasticity. H) Synthesis of new proteins is needed when LTP or LTD lasts for more than a few hours. Novel gene expression through the nucleus involves the cAMP-dependent pathway, of which PKA directly acts on the AMPA receptor in LTP expression. PKA activates a signalling cascade that leads to the expression of new transcripts which after translation contribute to the long-term expression of synaptic plasticity. I) The MAPK pathway is strongly implicated in mGluR-dependent LTD. Using this pathway, proteins are synthesized locally. J) The kinase PKMζ maintains AMPARs inserted via LTP and aids in memory retention. PKMζ inhibition can erase LTP and gained memory days after induction. K) In synaptic plasticity, BDNF can alter the synapse structure to enforce long-term changes in synaptic strength. NO: nitric oxide; ECs: endocannabinoids; mGluR: metabotropic glutamate receptors; BDNF: brain-derived neurotrophic factor; MAPK: Mitogen-activated protein kinase; PKMζ: protein kinase M zeta. For more detailed description, see source of the figure: [57].

S220's structure name is 8-benzylthioadenosine- 3', 5'- cyclic monophosphorothioate. It has a half maximal effective concentration (EC50) score of 0.1µM, which is 18-fold higher than that for cAMP (1.8µM) for EPAC2[72]. S220 is hypothesized to improve memory retrieval, but not memory acquisition nor consolidation, through EPAC2 activating GluA2/3 AMPARs, which in turn will activate NMDARs and induce Ca^{2+}-dependent memory and learning signalling cascades to occur.

Aim

In summary, this study consists of two aims regarding first, TNFR2 and its STAR2 agonist, and second, EPAC2 with its activator S220. The first part of the study focuses on answering the research question: "What is the effect of TNFR2 agonist STAR2 on AD pathology in a humanized J20 mouse model?", where we hypothesize STAR2 to reduce AD pathology and improve memory and learning behaviour by stimulating neuroprotective properties through activating

TNFR2, without interfering with TNFR1 signalling.

The second part of our study aims to answer the question: "What is the effect of S220, a cAMP analogue, on improving impaired memory retrieval by EPAC2 activation in acute and chronic AD mouse models?". Here we hypothesize the S220 compound to show improved memory retrieval in both a chronic and acute mouse model, on basis of the behavioural experiments Morris water maze (MWM) and contextual fear conditioning (CFC), compared to a PBS control group. Our chronic AD mouse model means to evaluate the long-term effect of the S220 compound on AD pathology, and the acute AD mouse model is used to study the different memory stages (acquisition, consolidation, and retrieval) to map the memory mechanism.

Materials and methods

Animal models, caretaking, and behavioural test preparation

For the STAR2/TNFR2 study, C57BL/6J wild-type mice had the extracellular part of human TNFR2 knocked-in (kihuTNFR2), where it was fused to the transmembrane and intracellular part of mouse TNFR[39]. This homozygous kihuTNFR2 strain was crossbred with transgenic hemizygous J20 B type mice to create a homozygous kihuTNFR2 x hemizygous J20 mouse model, of which only male mice were used. Transgenic J20 B, or simply J20 mice have two mutations (Indiana and Swedish) causing APP production in the mouse brain, providing the AD pathogenesis in these mice[41]. J20 mice were used for the chronic model in the S220/EPAC2 study, and C57BL/6J mice for the acute mouse model. Apart from C57BL/6J mice, in heterozygous offspring were used and confirmed by genotyping (not discussed). Also, only male mice were used and housed alone or with up to 5 mice in one cage, depending on the amount of offspring in the same litter meeting our requirements. Food (standard chow) and water was given *ad libitum* throughout the experiments and water was refreshed every week. Cages were cleaned once every one to two weeks. Cages were provided with floor-covering and nesting material. Enrichment consisted of 1-2 cardboard rolls. Day/night cycle was 12h/12h with change at 07:00h and 19:00h. Room checks were performed daily by checking food and water levels, as well as mice behaviour and welfare. Upon the start of the STAR2/TNFR2 study's behavioural experiments mice were housed individually and body weight was measured every week. For the S220/EPAC2 study, mice were not individually housed, but body weight was measured every day upon injection administration.

Humane endpoints consisted of losing >15% of original body weight (starting weight measured at beginning of injection and behavioural testing), alteration of behaviour such as hunched back, posture, fur, or alopecia, signs of illness and tumours, incorrect cannula placement, excessive bleeding through surgery, and finally health problems witnessed in post-operative recovery.

Mice were habituated in the room of testing, where they were handled by the researcher for 2min on the last 5 consecutive days prior to behaviour tests started. C57BL/6J mice underwent stereotactic surgery (not discussed) to install the double guide cannula for IH injection. After surgery, mice were housed individually in a clean cage with food and water ad libitum, and given 7 days (or more if needed) to recover. After surgery, body weight was measured daily and when a decrease of ≥0.5gr of body weight was witnessed over a 24h period, 5mg carprofen per 1kg body weight was administered subcutaneously (SC) as analgesia. On the first day after surgery, carprofen was administered regardless of (amount of decreased) body weight.

Animal care and experiment procedures were in concordance with the regulations of the University of Groningen ethical committee for the use of experimental animals.

Compound administration

75µg of STAR2 compound (dissolved in 200µl PBS) was administered to 6 months old kihuTNFR2 x J20 mice through intraperitoneal (IP) injections twice per week for 6 consecutive weeks.

After stereotactic surgery, 5-6 months old C57BL/6J mice received either 0.6µl PBS (0.3µl/hemisphere; not discussed) or 30pmol Aβ (0.6µl total, 0.3µl/hemisphere) IH injections to induce acute AD neuropathology 1h prior to the first of two days of CFC testing. The second IH injection (either 0.3µl PBS per hemisphere, or 300ng S220 dissolved in 0.3µl PBS per hemisphere) was given either 20min before CFC day 1, immediately after CFC day 1, or 20min before CFC day 2 to test memory acquisition, consolidation, or retrieval, respectively.

J20 mice between the age of 6-8 months received daily either 200µl PBS or 0.3mg S220 dissolved in 200µl in PBS via IP injections for 14 consecutive days.

Study time line

After 6 consecutive weeks of STAR2 (n=15) or PBS (n=15) administration, 7.5months old kihuTNFR2 x J20 mice were submitted to EPM, Y-maze, and MWM tests. After behavioural tests were completed, mice were sacrificed for brain, blood, and CSF collection for further 6e10, BACE1/6e10, and CD68/6e10 (data not presented) stainings.

After recovering from stereotactic surgery, C57BL/6J mice performed the two day CFC test. Subsequently, the mice received 0.3µl of methylene blue dye per hemisphere to determine correct positioning of the injection location of IH injections, after which the mice were immediately sacrificed through perfusion.

During the 14 consecutive days of IP injection with either S220 or PBS was administered to the J20 mice, on day 3-7, mice were habituated, and subsequently from day 8-17 mice performed the MWM experiment. Subsequently, perfusion occurred immediately after, with in half the brains paraformaldehyde (PFA) and the other half using saline for immunohistochemical staining or western blot analyses, respectively, for future research (not discussed).

Elevated plus maze

Anxiety behaviour was measured through the EPM behavioural test to ensure the tested compound itself does not influence mouse behaviour, making assumptions based on other data (more) accurate. Experiments were performed on a plus maze 50cm above the floor with opposing open and closed arms (Figure 8A). Mice were placed in the centre between all four arms and allowed to freely explore all arms for up to 8 minutes maximum. Percentages of cumulative time moved in all three zones (open arms, closed arms, centre) were provided by Ethovision software (Noldus, The Netherlands). An increased percentage of cumulative time spent in the closed arms indicates anxious behaviour.

Y-maze spontaneous alternation

The Y-maze spontaneous alternation experiment tested working memory by determining the amount of alternations in 10 minutes. The Y-maze consisted of three equal arms with walls in a 120 degree angle from one another, joined together at the centre triangle where the mice were placed at the start of the experiment (Figure 8B). Each arm was given a letter (A-C) and the mice were left to explore the entire maze freely. Alternation percentage was calculated by the formula: $\frac{number\ of\ triads}{total\ amount\ of\ arm\ entries-2} \times 100$. One triad is considered the consecutive order of three entries, withing the larger amount of entries, of which all three arm letters are different. The experiment was recorded by Ethovision software (Noldus, The Netherlands), and entries and alternation percentage were scored manually from the recordings by the researcher. Mice were scored to have entered an arm when all four limbs have crossed the

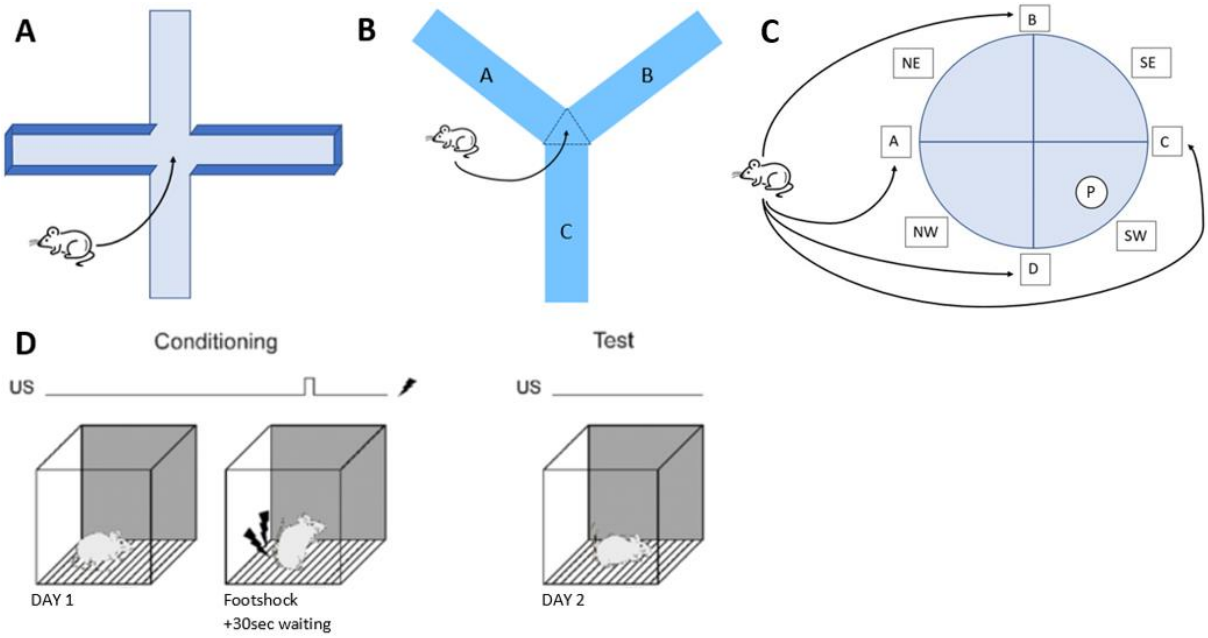

Figure 8 Behavioural experiments performed on kihuTNFR2 x J20 mice (A-C), J20 mice (C), or C57BL/6J mice (D). A) Elevated plus maze (EPM), consists of two closed and two open arms with a centre square connecting the arms. B) Y-maze spontaneous alternation; arms are given a letter for scoring (A, B, and C). C) Morris water maze (MWM); NE, SE, NW, and SW correspond to the quadrants northeast, southeast, northwest, and southwest respectively. A-D are entry points for mice to be placed into the water, and P = platform. D) Contextual fear conditioning (CFC); US = unconditioned stimulus. Source of A-C: own figures; source of D: [95].

imaginary line between the centre triangle and the arm.

Morris water maze

The Morris water maze (MWM) tests spatial memory and learning by putting mice in a tub with white opaque water of 22-25°C facing the edge of the tub, which had an inner diameter of 155cm, for four times 2min a day for 8 out of 10 consecutive days (Figure 8C). During these first 8 days of training, mice needed to find a circular platform (P) hidden on 0.8-1.1cm below water level in the southwest (SW) quadrant, invisible to the mice, in order to escape the maze. Mice started from a different starting point (A-D) for each of the four trials, randomized every day. Interval time between trial sessions was ≥15min. If mice were unable to locate the platform within 120sec, they were guided towards the platform and escape latency was set at 120sec. Mice always remained on the platform for 20 sec to allow visual recognition of the area, before being placed back in their cage under a heat lamp. If necessary, the water was cleaned before the next trial commenced. Mice were considered outliers and removed for data analysis when they were unable to locate the platform for ≥6/8 training days (average escape latency of four trials/day = 120sec). This was the case for three of the 15 mice in both treatment groups in the STAR2/TNFR2 study. For the S220/EPAC2 study, two mice in the S220-treated group had to be excluded.

The last two days of the test were the probe trials, where the platform was removed and mice swam 100sec, starting from the position between A and B, after which they were taken out of the maze. Time spent in each quadrant (northeast (NE), southeast (SE), northwest (NW), and southwest (SW)), and times platform space crossed were analysed (Figure 8C).

Data was collected by a camera above the tub, connected to the Ethovision program which provided the data for analysis.

Contextual fear conditioning

Contextual memory and learning was measured through the contextual fear conditioning (CFC) behavioural test, where

mice were placed in a soundproof cage with an electricity-conducting floor panel and constant illumination (100-500lux) for 180 seconds on day 1 (Figure 8D). After 180sec mice received a footshock (0.7mA, constant current; unconditioned) for 2sec, and were taken out after 30sec to prevent aversive association with handing by researcher[54]. On day 2, mice were placed back in the cage without administered footshock, at which the freezing percentage was measured by Ethovision software (Noldus, The Netherlands) and used for analysis.

Mice perfusion and brain section collection

Mice were sedated and brains were collected through perfusion. Mice were perfused with 4% paraformaldehyde (PFA) in 0.1M phosphate buffer (PB), after which the brain was taken out and post-fixated in 4% PFA for 24 hours at room temperature (RT). PFA was washed out in 0.01M PB for 3 days. Subsequently, brains were put on 30% sucrose until sunken to prevent crystallization, and stored at -20°C.

Frozen brains were sliced into 20µm coronal sections using the Leica cryostat. Sections were stored in 0.01M PB + 0.01% sodium azide at 4°C. One brain of each treatment group in the STAR2/TNFR2 study was damaged during collection, reducing the group size to n=14 for both treatment groups.

Amyloid-beta plaques (6e10) staining

Plaque staining was performed on three free floating dorsal (and ventral) hippocampal sections of 20µm thick per mouse, by targeting Aβ with the monoclonal antibody 6e10 that binds to amino acids 1-16 of the Aβ protein[73]. All steps were performed on an orbital shaker, at approximately 100 rpm unless stated otherwise. Staining was performed by first washing the sections (always 3x 5min in 0.01M tris-buffered saline (TBS) (pH 7.4) at RT unless stated otherwise). Next, endogenous peroxidase activity was blocked by incubation in 0.01M TBS + 0.3% H_2O_2 at RT for 30min. Subsequently, another washing step and pre-incubation of 1h in 0.01M TBS + 0.1% Triton X-100 (TX100) (for permeabilizing) + 3% goat serum (for blocking) at RT followed. Then, primary antibody incubation was performed in 0.01M TBS + 0.1% Triton X-100 + 3% goat serum + 6e10 (1:2000 dilution) (BioLegend, Cat #803003, Lot #B225308) at 4°C for 3 nights. After another washing step (3x 10min), secondary antibody incubation was performed with 0.01M TBS + 1% goat serum + goat anti-mouse antibody (dilution 1:400) for 2h at RT. Sections were washed (6x 5min) and the secondary antibody was visualized using its biotinylated properties by binding of Avidin-Biotin Complex (ABC) (VECTASTAIN ABC kit, Vector Laboratories, #PK6100). A and B of ABC were both used in a 1:500 dilution in 0.01M TBS for 1.5h at RT. After washing, diaminobenzidine (DAB) (Sigma Fast, Cat: D4418) was dissolved in demi water and added to the sections. 0.1% H_2O_2 in demi water was used to activate DAB. DAB exposure time was recorded and used for all sections. DAB activity was stopped by washing and sections were stored overnight at 4°C. The next day, sections were mounted onto glass slides in gelatine solution and dried overnight. Subsequently, section dehydration was performed using 5min incubation time of each of the following solutions: 100% ethanol (2x), 70% ethanol + 30% xylol (xylene), 30% ethanol + 70% xylol, 100% xylol (3x). Coverslipping was performed using dibutyl phthalate polystyrene xylene (DPX) as mounting media and dried overnight. Finally, slide edges were covered with transparent nail polish to preserve tissue staining and prevent oxidation. Slides were stored at 4°C.

Beta-secretase (BACE1/6e10) staining

Staining of β-secretase was performed by a β-site APP-cleaving enzyme (BACE1)/6e10 staining on three free floating dorsal (and ventral) hippocampus sections of 20µm thick per mouse. All steps were performed on an orbital shaker, at approximately 100 rpm. Staining started with washing the sections (always 3x 5min in 0.01M TBS (pH 7.4) at RT unless stated otherwise). Sections were added

to blocking solution (0.01M TBS + 0.1% TX100 + 3% bovine serum albumin (BSA)) for 1h at RT. Then, the primary antibodies rabbit anti-BACE1 (Cell Signalling Technology, Cat #5606S, Lot #5) (in dilution 1:200) and mouse anti-6e10 (BioLegend, Cat #803003, Lot #B225308) (in dilution 1:2000) incubated overnight at 4°C in fresh blocking solution. The next day, after washing, all steps were performed in the dark. The sections were incubated for 2h at RT in fresh blocking solution containing the fluorescent secondary antibodies anti-rabbit Alexa Fluor 488 (1:500) and anti-mouse Alexa Fluor 594 (1:500). Subsequently, sections were washed and mounted onto glass slides in 0.01M TBS. After 30-60min of drying, sections were coverslipped using mowiol antifade. When mowiol was dried, slide edges were covered with transparent nail polish to prevent loss of staining and stored at 4°C in the dark.

Phagocytic microglia (CD68/6e10) staining

Three free floating dorsal (and ventral) hippocampus sections of 20µm thick per mouse were used to stain phagocytic microglia by a CD68/6e10 staining. Staining protocol was similar to as described in the β-secretase staining, with the only alterations being: all washing steps are 6x 5min; 0.3% TX100 instead of 0.1%; used primary antibodies are rat anti-mouse CD68 (1:1000) (Bio-Rad, Ref #MCA1957GA, Lot #152755) and mouse anti-6e10 (1:2000) (BioLegend, Cat #803003, Lot #B225308); secondary antibodies used are donkey anti-rat Alexa Fluor 488 (1:500) and donkey anti-mouse Alexa Fluor 555 (1:500). Data of this staining is not presented due to time issues.

Microscopy

After sections were stained, pictures were taken using the LASX software and a Leica microscope using a 10x (6e10, BACE/6e10) and 20x (CD68/6e10) magnification for taking pictures with the navigator tool. Image analysis was completed by using ImageJ/Fiji software where percentages of stained tissue were determined.

Statistics

Data analysis was performed using Excel, SPSS version 28.0.0.0 (190), and GraphPad Prism version 8.0.1. Shapiro-Wilk tests were used to determine normality scores, and indicated the use of either parametric ($p>0.050$) or non-parametric tests ($p<0.050$), such as unpaired t-tests, and Mann Whitney tests respectively. Significance of data containing two or more factors was determined using a two-way AVONA repeated measures. Significance level was set at $p=0.050$.

Results

Anxiety levels are not altered in STAR2-treated group

After six consecutive weeks of daily intraperitoneal injections with either STAR2 or PBS, kihuTNFR2 x J20 crossbreed mice first performed the elevated plus maze test to determine if STAR2 influenced anxiety levels, and therefore mouse behaviour (Figure 9). The maze was divided into three different zones, the open arms, closed arms, and centre square. No significant difference was witnessed in time

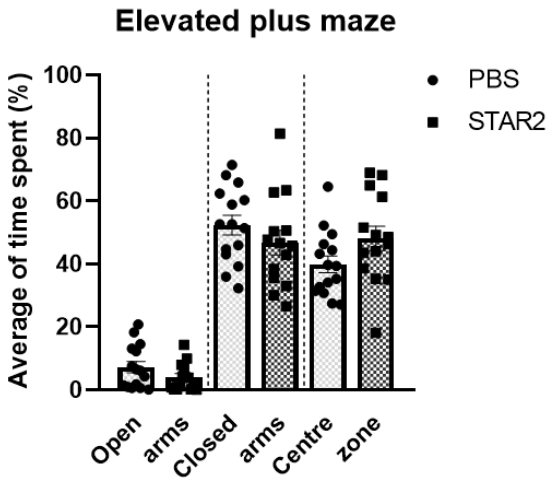

Figure 9 Elevated plus maze measured anxiety levels in treated group (STAR2; n=15) versus control group (PBS; n=15). Time spent in the maze was divided over three zones: open, closed, and centre. Data was acquired by Ethovision software. Data is considered not significant (p=0.2103) by two-tailed unpaired t-test. Error bars are standard error of the mean (SEM). Analysis was performed using GraphPad Prism.

spent in open (unpaired two- tailed t-test: p=0.1438; two-tailed Mann Whitney test: p=0.2012), closed (unpaired two- tailed t-test: p=0.2781), or centre (unpaired two-tailed t-test: p=0.0852) zones between treatment groups, indicating STAR2 treatment does not influence anxiety behaviour.

STAR2 treatment has no (significant) impact on working memory

Second, the kihuTNFR2 x J20 crossbreed mice were subjected to the Y-maze spontaneous alternation test to determine potential influence of STAR2 treatment on working memory. Working memory functions are based in the prefrontal cortex and the hippocampus[74], with our mouse model only developing AD symptoms in the latter region relating to this experiment. In our experiment, no (significant) difference is witnessed between the STAR2-treated group and PBS control group (Figure 11). This potentially limits STAR2's effectiveness to the hippocampal regions, without affecting the prefrontal cortex region and its functions. However, the impact of these observations is limited as the mouse model does not display AD pathology in the prefrontal cortex to the same extent as is witnessed in the hippocampus.

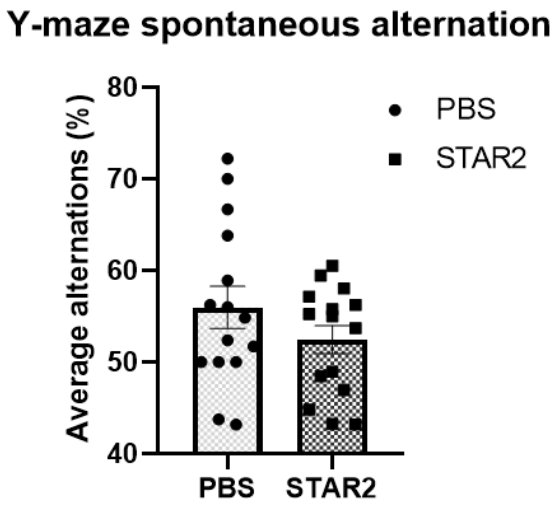

Figure 11 Y-maze spontaneous alternation assessed working memory in mice both treatment groups: PBS (control group; n=15) and STAR2 (treated group; n=15). Data from an unpaired t-test is considered not significant (p=0.2103). Error bars are standard error of the mean (SEM). Analysis was performed using GraphPad Prism.

Intraperitoneal STAR2 injections in kihuTNFR2 x J20 crossbreed mice significantly improve spatial memory and learning

After the EPM and Y-maze, the kihuTNFR2 x J20 crossbreed mice started with the Morris water maze experiment on the third day after the last IP injection was given. In the MWM experiment, which tests learning and spatial memory, latency to the platform was measured during the eight days of training (Figure 10)**.** Outlying mice were removed from the MWM data pool for this graph and further data as well (Figure 13 and Figure 12). Displayed data shows a clear significant trend (p=0.0123) for STAR2-treated mice to have a lower latency to find the platform. This implies STAR2 treatment to have a positive impact on spatial memory and learning.

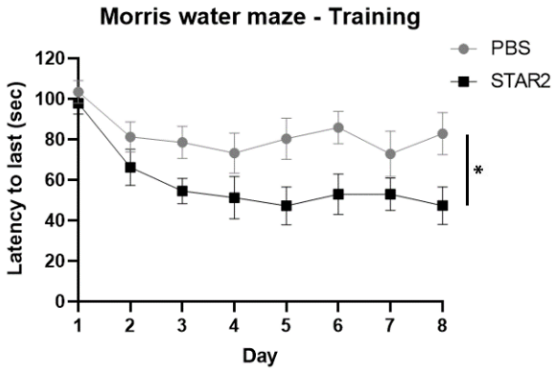

Figure 10 Morris water maze (MWM) training days (day 1-8) shows the STAR2-treated group (n=12) to find the platform quicker than the control group (PBS; n=12). A two-way analysis of variance (ANOVA) repeated measures showed significance comparing both graphs (p=0.0123). Error bars are standard error of the mean (SEM). Analysis was performed using GraphPad Prism.

After the eight days of training, mice were subjected to the probe trials on day 9 and 10 of the experiment, where the platform was removed from the maze and mice swam a total of 100sec once. Data shows a significant increase in time spent in the target quadrant (SW) for the STAR2-treated mice compared to the PBS control group on both day 9 (p=0.0156) and 10 (p=0.0154), indicating towards improved memory in the STAR2-treatment group (Figure 13).

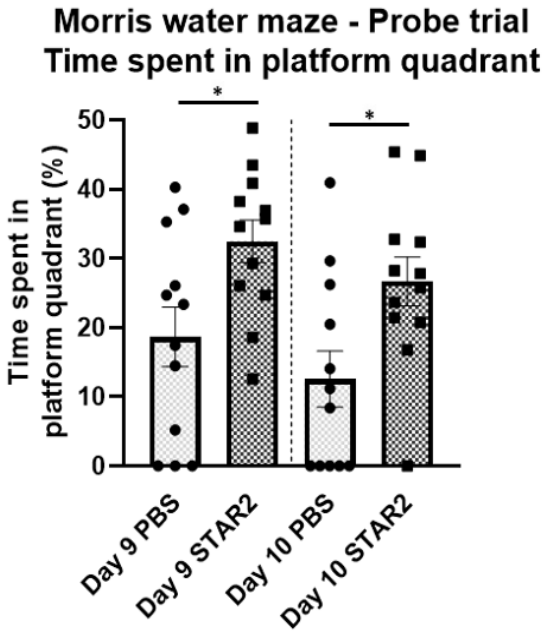

Figure 13 Morris water maze probe trials (day 9 and 10), time spent in the target quadrant (southwest). For MWM test set-up, see Figure 8C. Freezing percentage ("Time spent in platform quadrant (%)") determined spatial memory and learning level, with significantly higher percentages for the STAR2-treated group (n=12) compared to the PBS control group (n=12) on both day 9 (p=0.0156) and 10 (p=0.0154). Data was analysed using unpaired two-tailed t-tests in GraphPad Prism. Displayed error bars are standard error of the mean (SEM).

Data from the probe trials regarding the frequency of platform showed the STAR2-treated group to have a higher frequency in platform crossings than the PBS control group on both day 9 (p=0.1187) and day 10 (p=0.1748), though not significant (Figure 12). This unsignificant data implies STAR2 to have a positive effect on spatial memory and learning behaviour tested in the MWM experiment.

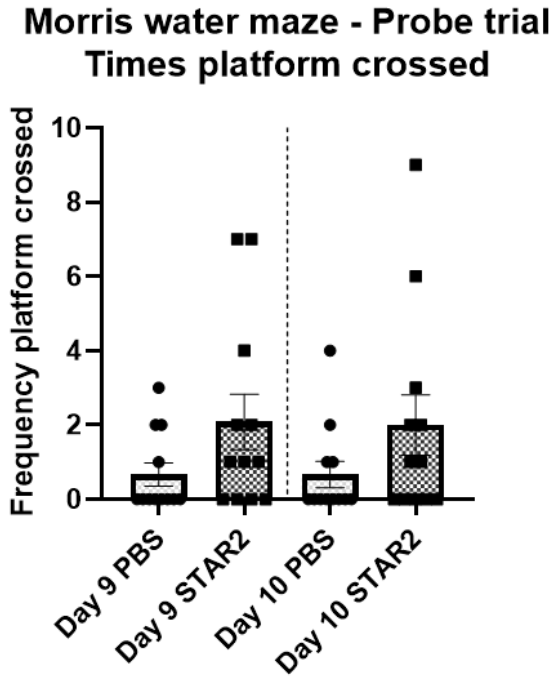

Figure 12 Morris water maze probe trials (day 9 and 10), times the platform area was crossed over. "Frequency platform crossed" determined spatial memory and learning level, with unsignificant higher scores from the STAR2-treated group (n=12) compared to the PBS control group (n=12) on both day 9 (p=0.1187) and 10 (p=0.1748). Data was analysed using two-tailed Mann Whitney tests in GraphPad Prism. Displayed error bars are standard error of the mean (SEM).

STAR2 significantly decreases Aβ plaque accumulation in hippocampus and cortex

Staining was performed on dorsal hippocampal (and ventral) sections from the kihuTNFR2 x J20 crossbreed mice's brains (Figure 16**,** top row). Aβ plaque accumulation in the hippocampus and cortex showed a significant decrease in STAR2 treated mice compared to the PBS control group (Figure 14A and C), indicating its function in reducing one of AD's important pathological hallmarks. Reduction of Aβ plaque accumulation in the corpus callosum was witnessed in the STAR2-treated group, though not significant (Figure 14B).

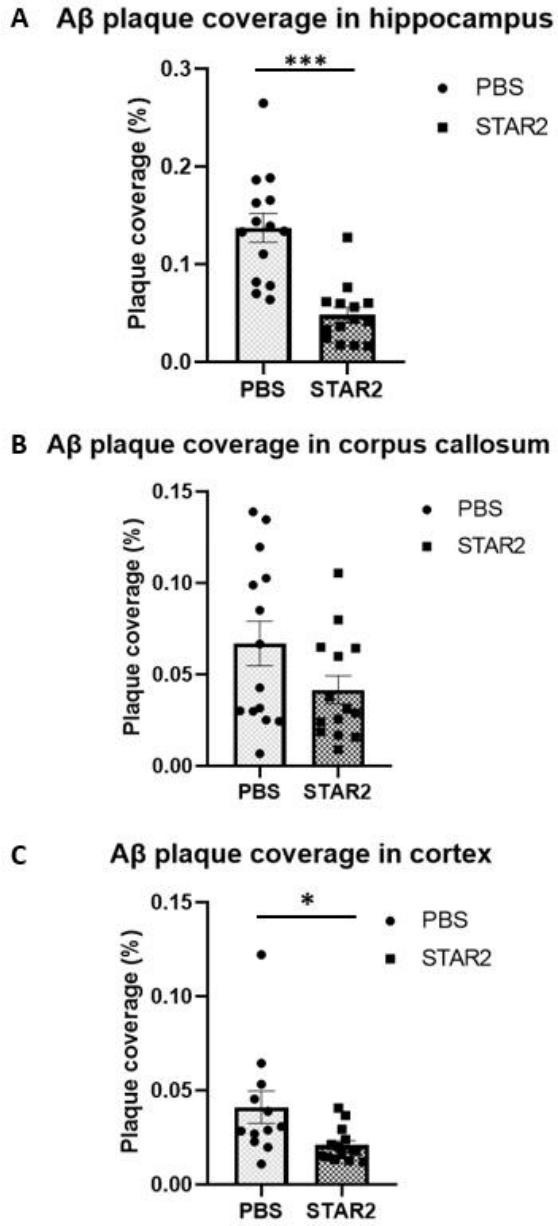

Figure 14 Amyloid beta (Aβ) plaque (6e10) staining was performed on free floating dorsal (and ventral) brain sections of both control (n=14) and STAR2-treated mice (n=14). Hippocampus (A), corpus callosum (B), and cortex (C) were analysed and show decreased plaque coverage in treatment group. P-values for A, B, and C, are p<0.0001, p=0.0895, and p=0.0127, respectively. Data was acquired through unpaired t-test (A, B), and Mann Whitney test (C). Error bars are standard error of the mean (SEM). Analysis was performed using GraphPad Prism.

STAR2 unsignificantly reduces beta-secretase levels in hippocampus, but not in corpus callosum

The second staining on the kihuTNFR2 x J20 crossbreed mice's brains was that of the fluorescent beta-secretase (BACE1/6e10) staining (Figure 16**,** bottom row). Data shows an unsignificant decrease in β-secretase levels in STAR2-treated mice in both the hippocampus and corpus callosum (p=0.8707)

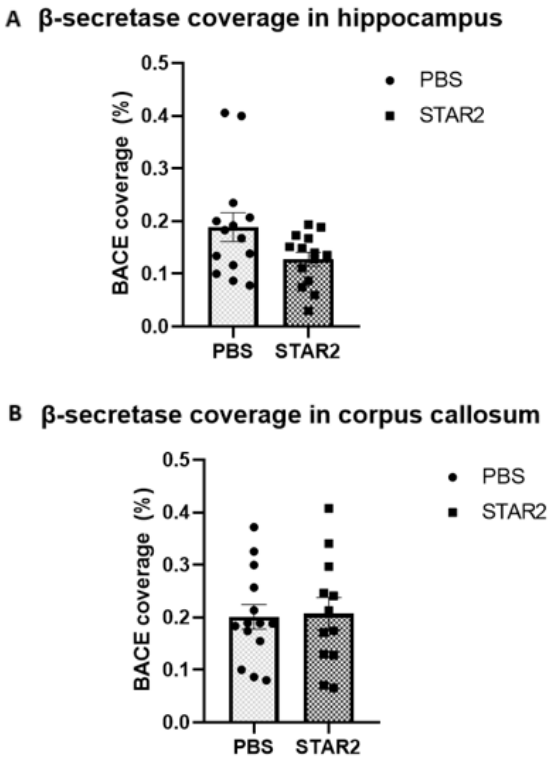

Figure 15 BACE1 staining stained beta(β)-secretase in free floating dorsal (and ventral) brain sections of both control (n=14) and STAR2-treated mice (n=14 in hippocampus; n=12 in corpus callosum). Hippocampus (A) data shows unsignificant (p=0.0548) decrease in β-secretase levels in the STAR2-treated group compared to control group. Differences in the corpus callosum (B) were not present and data was not significant (p=0.8707). Data was acquired through unpaired t-test (A, B). Error bars are standard error of the mean (SEM). Analysis was performed using GraphPad Prism.

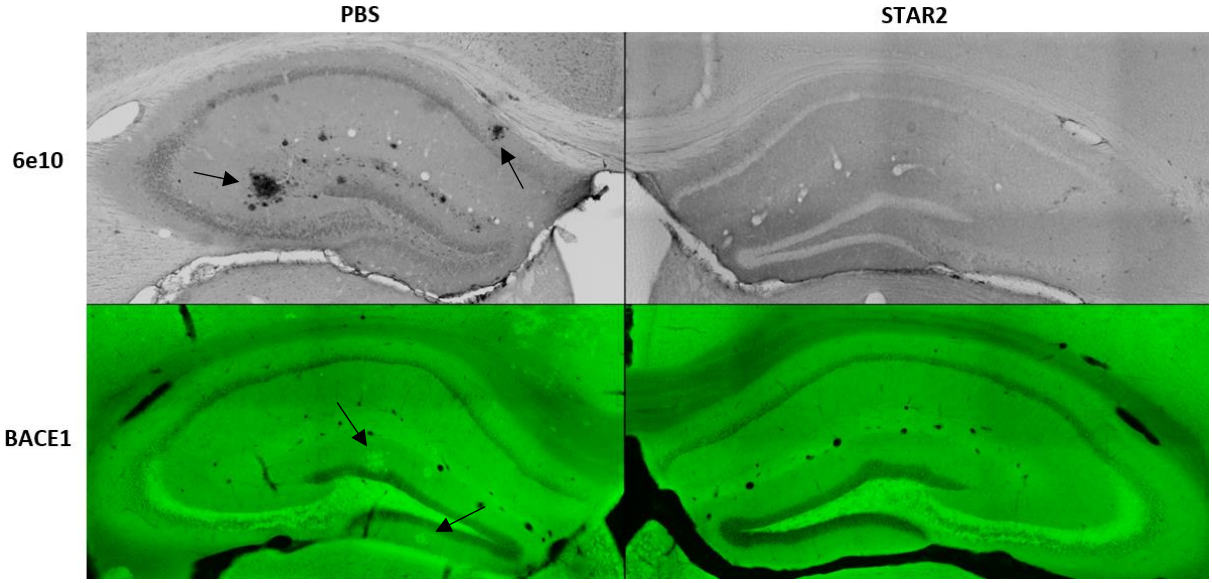

Figure 16 Staining of Aß plaques (6e10) and ß-secretase (BACE1) on dorsal (and ventral) kihuTNFR2 x J20 crossbreed mice's brain sections. Mice received different treatments, being PBS for the control group, and STAR2 as actual treatment compound. Aß plaques are visible as black stains made up of tinier black specks joined together (arrows)). ß-secretase proteins are stained as light green donut-shaped circles (arrows). The brain's pyramidal cells and hilus stain darker and lighter as 'false' positive signal in the 6e10 and BACE1 staining, respectively. Displayed brain sections show only the hippocampus and corpus callosum area, where staining data also consisted of cortex values, but of which no figure is displayed here.

(Figure 15A and B). Though, data was nearly significant in hippocampus (p=0.0548), implying an effect of STAR2 on β-secretase levels to exist.

S220 unsignificantly stimulates memory retrieval in chronic J20 mouse model

For the second part of our study, we evaluated the effect of EPAC2 activation through the S220 compound. For the chronic mouse model we were able to perform pilot studies to evaluate the long-term effect of S220 on a AD mouse model. The performed MWM experiment, used to test spatial memory and learning, showed a lower time needed to find the platform ("Latency to last (sec)") for S220-treated mice, though unsignificant (p=0.7357; Figure 17).

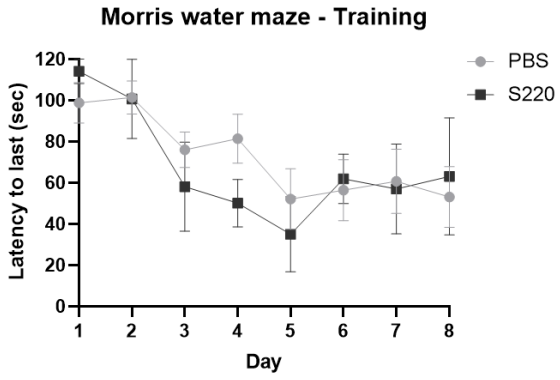

Figure 17 Morris water maze (MWM) training days (day 1-8) shows the S220-treated group (n=3) to find the platform the last time ("Latency to last(sec)") generally quicker than the control group (PBS; n=5), though unsignificant. A two-way analysis of variance (ANOVA) repeated measures was performed on the data (p=0.7357). Error bars are standard error of the mean (SEM). Analysis was performed using GraphPad Prism.

Data regarding the probe trials are not discussed, as no trend and no significant data was obtained.

EPAC2 activation by intrahippocampal S220 injections in acute J20 mouse model significantly stimulates contextual memory and learning

Contextual fear conditioning experiments were performed to test contextual memory and learning in the acute AD mouse model. This was performed to map memory retrieval in treated (S220; n=5) and control (PBS; n=4) mice (Figure 18). Data shows S220-treated mice ("Aβ + S220") to have a higher freezing percentage ("Time frozen (%)") compared to the control group ("Aβ + PBS"). An unpaired two-tailed t-test confirms the data to be significant (p=0.0381), implying S220 treatment to rescue Aβ-dependent impaired memory retrieval.

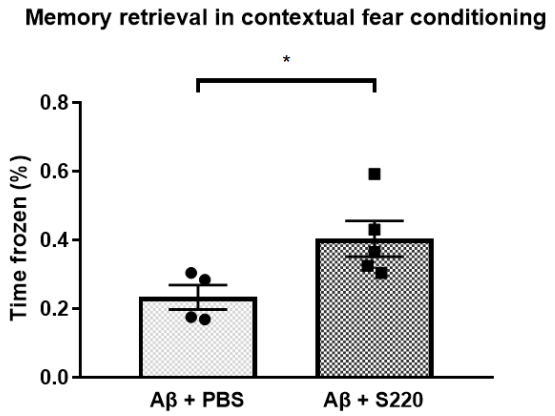

Figure 18 Contextual fear conditioning (CFC) experiments show a significantly higher freezing percentage ("Time frozen (%)") in the S220-treated group (n=5) compared to the PBS control group (n=4) using an unpaired t-test (p=0.0381). Error bars are standard error of the mean (SEM). Analysis was performed using GraphPad Prism.

Discussion

This study aimed to evaluate the effect of TNFR2 agonist STAR2, and EPAC2 activator S220, on Alzheimer's disease mouse models using immunohistochemical and behavioural analyses.

Concerning the behavioural experiments of the STAR2/TNFR2 study, the EPM was performed to test anxiety in mouse behaviour in order to determine potential influence of the STAR2 compound on other behaviour experiments' data. EPM data showed STAR2 to have no statistically significant impact on mouse anxiety behaviour, as no significant difference was found between control (PBS) and treated (STAR2) group. This indicates that the varieties in collected data from the Y-maze and MWM can be attributed to the difference in treatment. Though, e.g. observer bias is always a potential threat that needs to be pointed out in analysis of experiments which require animal handling and where manual scoring by the researcher is needed (Y-maze) instead of software being used (EPM and MWM)[75]. The Y-maze experiment was performed blinded to the researcher, but manual analysis of the recordings was not blinded and in so doing vulnerable to observer bias when data was scored. Though the impact of this bias is most likely negligible as the Y-maze data was not significant, nor showing a clear trend; it is a note for future experiments vulnerable to this bias type. Single or double (preferable) blinding the researcher before the analysis of experiments vulnerable to observer bias has shown to increase credibility of study conclusions[76].

The Y-maze was performed to determine possible influence of our STAR2 compound on working memory, located in the prefrontal cortex and hippocampus. The former area was not possible to examine in our study as this area is not affected by Aβ plaques deposition ad much as is in the latter region. Also, mice, and other rodents, do not have a similar prefrontal cortex as primates. Though other regions can be attributed to similar functions[77,78], how these should be translated back to human AD neuropathology leaves weak conclusions to be drawn based on our non-significant Y-maze data. STAR2-treated mice seem to show a lower alternation percentage, compared to the control group, which could indicate a decrease in working memory through STAR2 treatment. However, this conclusion does not hold very well as the witnessed difference (apart from being unsignificant) is very small, and TNFR2 is mainly expressed in immune and endothelial cells[11]. Taking this into account, it is also unlikely that, as the prefrontal cortex is altered in AD brains in late stages of disease development (with severe dementia symptoms)[79], that STAR2 treatment would have negatively affected similar prefrontal-functioning brain regions in mice and diminished working memory functions when mice were used only between 6 and 8 months of age. A study by Ameen-Ali et al. showed onset of Aβ plaque formation and co-localization of microglia and astrocytes to start from 6 months onward in J20 mice, whereas the glial cell's reactivity increases more severely after 9 months[80]. This implicates the unlikeliness of STAR2 to have been able to affect prefrontal cortex's working memory function in our study, as disease progression may not have advanced thus far yet in our mice

's brains. Though, a similar study by Chavant et al. using imipramine, a TNF-α production-inhibitor in microglia, showed significant rescue of impaired working memory in male Swiss mice injected with Aβ25-35 peptides[81]. The results of this comparable study stimulates a repetition of our Y-maze experiments, to investigate whether potential significant memory-rescuing results with STAR2 treatment can be retrieved after all, or to confirm its non-existing relation.

The MWM experiment showed improved spatial memory and learning in the STAR2-treated group, empowering its potential to decrease AD neuropathology. A clear correlation is seen in STAR2 treatment and reduced escape latency (Figure 10). This trend continued throughout the probe trials where STAR2-treated mice spent significantly more time looking for the platform in the corresponding quadrant (Figure 13), as well as crossing the platform space with higher frequency, though the latter was not significant (Figure 12). Palop et al. reported that J20 mice between the age of 6 and 9 months in general perform badly in MWM and probe trials of other special location retention tests, in line with our findings of the control group[82]. Chen et al. went as far as to show 3 months old PDAPP mice displaying impaired spatial memory in MWM[83]. These studies validate the positive outcome witnessed in our treatment group compared to existing untreated comparable mouse models. As AD research in relation to STAR2 treatment is as good as non-existent, our results could not be validated by papers matching our set-up related to the compound. However, the earlier mentioned study by Chavant et al. received promising similar results in using imipramine to rescue Aβ plaque accumulation-induced cognitive impairments in MWM tests as well[81], allowing our research's credibility to be validated to matching standards.

Subsequent to the behavioural experiments, the immunohistochemical analyses were executed on STAR2 and control group mice brains sections. The 6e10, BACE1/6e10, and CD68/6e10 immunohistochemical stainings were performed to determine Aβ plaque, β-secretase, and phagocytic microglial levels, respectively, with brain regions of interest being the hippocampus (subregions: CA1, CA3, and DG), CC, and cortex. The 6e10 staining showed significantly and not-significantly decreased levels of Aβ plaque accumulation in the STAR2-treated group compared to the PBS control group in the hippocampus ($p<0.0001$), CC ($p>0.050$; not significant), and cortex ($p<0.050$). This indicates STAR2 to rescue memory, learning, and possibly other higher brain functions attributed to the hippocampus and cortex by removing or preventing Aβ plaque accumulation to occur, a hallmark of AD. These impairments in higher brain functions correspond with AD symptoms witnessed in our untreated mice. Decreased memory (retrieval) and learning functions being common symptoms describing dementia, relates STAR2 functions back to potential in human AD pathology[1,4]. Regarding the 6e10/Aβ plaque staining, a study by Fabbro et al. observed similar results relating to the clearance of Aβ plaque accumulation in their neuroserpin-deficient J20-transgenic mice, compared to 'normal' J20-transgenic mice[84]. Plasminogen activators, thought to promote proteolytic cleavage and clearance of Aβ plaques from brain tissue, reducing AD pathology, are inhibited by neuroserpin[84]. A different study, by McAlpine et al., where TNFR1 was less stimulated due to solTNF inhibition through chronic infusions of dominant negative TNF inhibitors, indicated a decrease in 6e10-immunoreactive protein stains in the hippocampus, cortex and amygdala, not mentioning the corpus callosum[85]. These results, similar to our own regarding Aβ plaque decrease in hippocampus and cortex, strengthen our findings that TNF-α-related treatments indeed impact AD pathology towards a positive outcome in handling AD. Though our 6e10 staining data shows significance (apart from CC data), its validity could be questioned as staining data

was not scored by specifically designed software, but by a researcher using ImageJ to produce observer-scored values with this program. As mentioned earlier, when not blinded to the different groups, the researcher can consciously and subconsciously influence scored data, making it biased. This can also be the case for all staining data as no software was used here, and thus remains vulnerable to this bias. Though it is possible, this scenario is unlikely, as much data was produced and analysed which would mean a large number of staining images needed to be (seriously) biased in order to produce a large enough factor to impact the data, observer bias is still a factor that is important enough to take into account when validating data credibility. Apart from this bias, data could also have been influenced by the fact that most of the control group stainings were performed by one researcher, where the most of the treated group were performed by another researcher on a different time and day. However, both procedures were the same and supervised by the same supervisor, making this data being false positive unlikely. Therefore, it can be assumed that TNFR2 stimulation rescues neurons from degeneration, and protects against Aβ plaque deposition.

Results witnessed in the BACE1/6e10 staining, where β-secretase was stained fluorescently together with Aβ plaques, revealed no significant reduction in β-secretase levels in the STAR2 treated group compared to control. Images where the stainings are overlapping show Aβ plaques to be surrounded by β-secretase (data not displayed). Data was obtained from the hippocampus and CC, but not from the cortex as stained sections were too damaged to provide accurate values for this region. Though not significant, a decreasing trend of the treated group is witnessed in the hippocampus, which according to a study from Yamamoto et al. can be linked back to TNF-α levels. TNF-α can activate astrocytes which in turn stimulate β-secretase[86]. Another study, by Jiang et al., showed the promotor region of BACE1 contains NF-κB binding sites, possibly explaining this link as TNF-α can induce the NFκB pathway[87]. Therefore, it is assumable that a decrease in TNF-α levels may also decrease β-secretase levels, and in so doing reduce Aβ plaque accumulation, as pro-inflammatory signalling through TNFR1 would be reduced when TNF-α levels decrease. This correlation is also supported by Jiang et al. having found as well that overexpression of TNFR2 inhibited BACE1 transcription by limiting NF-κB nuclear translocation[87].

When looking into affected phagocytic microglia (CD68/6e10 staining, results missing) levels through TNF-α meddling, both a decrease or increase in phagocytic microglia levels can be expected. Time issues lead to this data not having been analysed yet and has therefore also not been added to this report. Though, literature studies may give some insight regarding plausible expectations. Yamamoto et al. observed that co-stimulation of IFN-γ and TNF-α in Swedish mutant APP transgenic mice lead to suppression of Aβ clearance by (phagocytic) microglia[86]. However, depending on one's assumption on whether the amyloid cascade theory or the microglial dysfunction hypothesis is most probable, an increase in phagocytic microglia levels can also be expected, with our Aβ plaque levels being lower in the STAR2-treated group than in the control group. For example, the study of Jordão et al. witnessed reduced Aβ plaque levels after their transcranial focused ultrasound treatment increased localized permeability for antibodies to pass the BBB, but also witnessed increased microglia levels with higher Aβ concentrations inside the cytosol[88]. This result implies that decreased Aβ plaque levels can accompany elevated phagocytic microglia levels, by microglia performing their phagocytic function in AD pathology.

In our S220/EPAC2 study, the chronic J20 mouse model had the function to evaluate the long-term effect of EPAC2 activator and cAMP

analogue S220 on AD pathology. The acute model aimed to study the different memory stages (acquisition, consolidation, and retrieval) to map the memory mechanism, and potential impact of our compound. Data of the chronic model's pilot study showed no significance, though a trend in favour of the S220-treated group showing a lower escape latency ("Latency to last (sec)") compared to the control group was witnessed. This implies a lesser, or unaffected memory retrieval function by Aβ plaques due to S220 rescue, which has yet to be further investigated. Regarding the MWM test, two out of the five mice in the S220-treated group in this pilot study were considered outliers and excluded from the data. Mice were considered outliers when six or more from the eight days of training showed an averaged escape latency of 120sec, meaning the mice did not find the platform once out of the four attempts that day. This behaviour can be attributed to thigmotaxis, a well-known phenomenon in rodents performing water-maze tests. Using special software (unavailable to us), thigmotaxis could be detected early on in the training days with calculating high certainty of thigmotaxis continuation as the MWM experiment progresses to the probe trials[89]. External factors such as (too) bright light can also have an influence on inducing thigmotaxis behaviour, and enhancing escape latency according to a study by Huang et al.[90], providing possible factors that may need to be reinvestigated or adjusted before continuation of the subsequent pilot studies and main study (not further discussed) using MWM. In a previous pilot study the MWM experiment was performed similar to execution of the MWM in the STAR2/TNFR2 study regarding the timing of IP injection and MWM (Appendix 2: Supplementary data of pilot study of chronic AD mouse model testing S220 effectiveness on memory retrieval using Morris water maze, Figure 19). This data showed it was potentially possible that the effect of S220 was diminished after the third day of MWM, as treatment injections stopped 1 day before MWM began. Therefore, the timeline was moved up to have mice receive IP injections containing either PBS or S220 on day 1-14, habituation from day 3-7, and the MWM experiment from day 8-17, having 7/10 MWM days overlapping with compound (or PBS) administration (Figure 17). Though still in favour of S220 treatment, differences in the trends are witnessed when comparing Figure 17 and Figure 19. This could be due to the time line being moved up which prevents potential loss of compound effectiveness, but the change in researcher performing the test can also be the cause, as well as the impact of a low animal number for the treatment group due to outliers (n=3 for S220 group; n=5 for PBS group). The latter situation leaving individual behaviour to have a high impact on group average, making results seem potentially skewed. Future power analyses will determine proper group mouse numbers to reduce individual mice impacting the data.

The acute model of the S220/EPAC2 study was to evaluate the effect of S220 on the three different memory stages (acquisition, consolidation, and retrieval). In this model C57BL/6J mice received IH injections containing either Aβ to induce AD pathology (or PBS as control) 1h prior to CFC testing on the first day, and a second injection containing either S220 (or PBS as control) to rescue impaired memory function on different time points corresponding to the tested memory stage. Data showed a significant effect ($p=0.0381$) of S220 treatment on freezing percentage ("Time frozen (%)"; Figure 18). This is in line with our hypothesis where we generally expected S220 to improve memory retrieval by activating EPAC2.

Finally, future studies can focus on evaluating the effect of STAR2 on different AD mouse models, such as mouse models expressing tau pathology. The Htau^{c} mouse, possibly derived from C57Bl/6, the similar mouse model used to create the kihuTNFR2 x J20 mouse model used for our study can be examined. In the Htau^{c} mouse model human tau is the promotor of the disease, which has its onset at 15 months and

shows pre-tangles at 9 months. This looks most similar to the kihuTNFR2 x J20 mouse model, where the knocked-in TNFR2 gene is also human[91]. Another candidate is the JNPL3 mouse, also possible to derive from C57Bl/6, though the promotor used is the mouse prion protein (PrP), and does not use human knock-ins. A positive use of this mouse model is the onset of the NFT at 9 months[92]. The earlier the onset of the disease, the lesser is needed to sustain the animal before it can be of use in animal experiments, also giving less pressure on the environment, and making this choice the more sustainable one based on animal care. After or instead of individual NFT mouse model experiments, one can also choose for a mouse model that has both Aβ and NFT expressed, to analyse a more complete picture of AD pathology in mouse models. For different options, this review by Chin gives a good overview of AD mouse model options[93]. Female mice can also be considered for future experiments, as in many AD mouse models they seem to be more susceptible to tangles and plaques onset, though it should be noted that not all phenotypes are aggravated more (quickly) in female mice. Every mouse model can show a gender-biased and different results, which should be thought of before choosing a new mouse model to experiment with[94]. Using female animal models should be well-thought through as changing hormone levels may influence study outcome. Future research can also entail executing the Y-maze test for the STAR2/TNFR2 study again as data may lead to significance with a larger group size, though the gain from such an experiment against animal welfare would have to be determined by an appropriate board specialized in such an ethical issue.

After having (optimized and) completed the necessary pilot studies for the chronic mouse model and after completing main study in both the acute and chronic mouse model in the S220/EPAC2 study, using a different mouse model can also be beneficial to research. Some mouse models solely expressing tau pathology displayed in Chin's review also show cognitive deficits, providing a solid future for continuing this research[93], where AD pathology might be diminished even better, though time will have to tell. In future studies further on the horizon, both STAR2 and S220 may be tested for treatment on human AD patients as is the ultimate goal of AD research. Though before such endeavours are taken, side effects should be mapped out well, as both TNFR2 and EPAC2 are expressed in other areas in the body apart from the brain, to prevent unnecessary detrimental effects on patients.

Conclusion

In conclusion, STAR2, a TNFR2 agonist, improves memory and learning in the humanized transgenic kihuTNFR2 x J20 crossbreed mouse model upon long-term IP injection (prior to behavioural testing). STAR2 significantly decreases AD pathology concerning Aβ plaque accumulation in hippocampus and cortex, though no such significant decrease was witnessed in β-secretase levels. This proves our hypothesis of STAR2 reducing AD pathology and improving memory and learning behaviour by stimulating neuroprotective properties through activating TNFR2, without interfering with TNFR1 signalling, to be in line with our recent findings. However, continued research is required in order to validate enhanced treatment possibilities for the STAR2 compound before human treatment can be considered.

Treatment with S220, a cAMP analogue and EPAC2 activator, shows a promising trend in rescuing impaired memory in the chronic AD mouse model (transgenic J20 mice), using MWM to test spatial memory and learning, though continuation of the study is needed to verify results significantly. In the acute AD mouse model, using C57BL/6J + Aβ IH injections, S220 administration significantly increased contextual memory and learning, indicating the potential of S220 in rescuing impaired memory retrieval function by AD pathology. However, continuation of the study

will provide a better insight into the effect of S220 on AD pathology and memory retrieval.

Acknowledgements

I would like to thank all of my supervisors, Prof. Dr. Ulrich L. M. Eisel, Natalia Ortí-Casañ and Tong Zhang for giving me this opportunity to learn from them and be allowed to be a part of their interesting and exciting research. I would also like to thank Wanda Douwenga for her personal support during my research project. I am happy to say I leave as a scientist with more knowledge and experience due to their time and effort in my education, for which I am grateful. I will look back happily on these 8.5 months of time spent under their supervision.

References

1. 2021 Alzheimer's disease facts and figures. *Alzheimer's & Dementia* **17**, 327–406 (2021).

2. Leng, F. & Edison, P. Neuroinflammation and microglial activation in Alzheimer disease: where do we go from here? *Nature Reviews Neurology* **17**, 157–172 (2021).

3. Puzzo, D., Gulisano, W., Arancio, O. & Palmeri, A. The keystone of Alzheimer pathogenesis might be sought in Aβ physiology. *Neuroscience* **307**, 26–36 (2015).

4. Thomas, S. A. Neuromodulatory signaling in hippocampus-dependent memory retrieval. *Hippocampus* **25**, 415–431 (2015).

5. Lopez, J., Gamache, K., Schneider, R. & Nader, K. Memory Retrieval Requires Ongoing Protein Synthesis and NMDA Receptor Activity-Mediated AMPA Receptor Trafficking. *Journal of Neuroscience* **35**, 2465–2475 (2015).

6. Breijyeh, Z. & Karaman, R. Comprehensive Review on Alzheimer's Disease: Causes and Treatment. *Molecules* **25**, 5789 (2020).

7. Morris, G. P., Clark, I. A. & Vissel, B. Inconsistencies and Controversies Surrounding the Amyloid Hypothesis of Alzheimer's Disease. *Acta Neuropathologica Communications* **2**, 135 (2014).

8. Briggs, R., Kennelly, S. P. & O'Neill, D. Drug treatments in Alzheimer's disease. *Clinical Medicine* **16**, 247–253 (2016).

9. Long, J. M. & Holtzman, D. M. Alzheimer Disease: An Update on Pathobiology and Treatment Strategies. *Cell* **179**, 312–339 (2019).

10. Vaz, M. & Silvestre, S. Alzheimer's disease: Recent treatment strategies. *European Journal of Pharmacology* **887**, 173554 (2020).

11. Ortí-Casañ, N. *et al.* Targeting TNFR2 as a Novel Therapeutic Strategy for Alzheimer's Disease. *Frontiers in Neuroscience* **13**, (2019).

12. Jankovska, N., Olejar, T. & Matej, R. Extracellular Amyloid Deposits in Alzheimer's and Creutzfeldt–Jakob Disease: Similar Behavior of Different Proteins? *International Journal of Molecular Sciences* **22**, 7 (2020).

13. Barbier, P. *et al.* Role of Tau as a Microtubule-Associated Protein: Structural and Functional Aspects. *Frontiers in Aging Neuroscience* **11**, (2019).

14. Michalicova, A., Majerova, P. & Kovac, A. Tau Protein and Its Role in Blood–Brain Barrier Dysfunction. *Frontiers in Molecular Neuroscience* **13**, (2020).

15. Venkatramani, A. & Panda, D. Regulation of neuronal microtubule dynamics by tau: Implications for tauopathies. *International Journal of Biological Macromolecules* **133**, 473–483 (2019).

16. Hayden, E. Y. & Teplow, D. B. Amyloid β-protein oligomers and Alzheimer's disease. *Alzheimer's Research & Therapy* **5**, 60 (2013).

17. Klein, W. L., Stine, W. B. & Teplow, D. B. Small assemblies of unmodified amyloid β-protein are the proximate neurotoxin in Alzheimer's disease. *Neurobiology of Aging* **25**, 569–580 (2004).

18. Siddiqi, M. K., Majid, N., Malik, S., Alam, P. & Khan, R. H. Amyloid Oligomers, Protofibrils and Fibrils. in 471–503 (2019). doi:10.1007/978-3-030-28151-9_16.

19. Chen, G. *et al.* Amyloid beta: structure, biology and structure-based therapeutic development. *Acta Pharmacologica Sinica* **38**, 1205–1235 (2017).

20. Morley, J. E., Farr, S. A., Nguyen, A. D. & Xu, F. What is the Physiological Function of Amyloid-Beta Protein? *J Nutr Health Aging* **23**, 225–226 (2019).

21. Brothers, H. M., Gosztyla, M. L. & Robinson, S. R. The Physiological Roles of Amyloid-β Peptide Hint at New Ways to Treat Alzheimer's Disease. *Frontiers in Aging Neuroscience* **10**, (2018).

22. Zhao, J., Deng, Y., Jiang, Z. & Qing, H. G Protein-Coupled Receptors (GPCRs) in Alzheimer's Disease: A Focus on BACE1 Related GPCRs. *Frontiers in Aging Neuroscience* **8**, (2016).

23. Siegel, G. *et al.* The Alzheimer's Disease γ-Secretase Generates Higher 42:40 Ratios for β-Amyloid Than for p3 Peptides. *Cell Reports* **19**, 1967–1976 (2017).

24. Barage, S. H. & Sonawane, K. D. Amyloid cascade hypothesis: Pathogenesis and therapeutic strategies in Alzheimer's disease. *Neuropeptides* **52**, 1–18 (2015).

25. Armstrong, R. A. What causes alzheimer's disease? *Folia Neuropathol* **51**, 169–88 (2013).

26. Castellani, R. J., Plascencia-Villa, G. & Perry, G. The amyloid cascade and Alzheimer's disease therapeutics: theory versus observation. *Laboratory Investigation* **99**, 958–970 (2019).

27. Streit, W. J., Khoshbouei, H. & Bechmann, I. The Role of Microglia in Sporadic Alzheimer's Disease. *Journal of Alzheimer's Disease* **79**, 961–968 (2021).

28. Hardy, J. A. & Higgins, G. A. Alzheimer's Disease: The Amyloid Cascade Hypothesis. *Science (1979)* **256**, 184–185 (1992).

29. Kwon, H. S. & Koh, S.-H. Neuroinflammation in neurodegenerative disorders: the roles of microglia and astrocytes. *Translational Neurodegeneration* **9**, 42 (2020).

30. Olmos, G. & Lladó, J. Tumor Necrosis Factor Alpha: A Link between Neuroinflammation and Excitotoxicity. *Mediators of Inflammation* **2014**, 1–12 (2014).

31. Clark, I. A. & Vissel, B. Amyloid β: one of three danger-associated molecules that are secondary inducers of the proinflammatory cytokines that mediate Alzheimer's disease. *Br J Pharmacol* **172**, 3714–27 (2015).

32. Clark, I. A. & Vissel, B. Therapeutic implications of how TNF links apolipoprotein E, phosphorylated tau, α-synuclein, amyloid-β and insulin resistance in neurodegenerative diseases. *British Journal of Pharmacology* **175**, 3859–3875 (2018).

33. Koenigsknecht-Talboo, J. Microglial Phagocytosis Induced by Fibrillar -Amyloid and IgGs Are Differentially Regulated by Proinflammatory Cytokines. *Journal of Neuroscience* **25**, 8240–8249 (2005).

34. Tansey, M. & McAlpine. Neuroinflammation and tumor necrosis factor signaling in the pathophysiology of Alzheimer's disease. *Journal of Inflammation Research* 29 (2008) doi:10.2147/JIR.S4397.

35. Hickman, S. E., Allison, E. K. & el Khoury, J. Microglial Dysfunction and Defective -Amyloid Clearance Pathways in Aging Alzheimer's Disease Mice. *Journal of Neuroscience* **28**, 8354–8360 (2008).

36. Dong, Y., Dekens, D., de Deyn, P., Naudé, P. & Eisel, U. Targeting of Tumor Necrosis Factor Alpha Receptors as a Therapeutic Strategy for Neurodegenerative Disorders. *Antibodies* **4**, 369–408 (2015).

37. Fischer, R., Kontermann, R. & Maier, O. Targeting sTNF/TNFR1 Signaling as a New Therapeutic Strategy. *Antibodies* **4**, 48–70 (2015).

38. Chopra, M. *et al.* Exogenous TNFR2 activation protects from acute GvHD via host T reg cell expansion. *Journal of Experimental Medicine* **213**, 1881–1900 (2016).

39. Dong, Y. *et al.* Essential protective role of tumor necrosis factor receptor 2 in neurodegeneration. *Proceedings of the National Academy of Sciences* **113**, 12304–12309 (2016).

40. Mucke, L. *et al.* High-Level Neuronal Expression of Aβ $_{1–42}$ in Wild-Type Human Amyloid Protein Precursor Transgenic Mice: Synaptotoxicity without Plaque Formation. *The Journal of Neuroscience* **20**, 4050–4058 (2000).

41. Tosh, J. L. *et al.* The integration site of the APP transgene in the J20 mouse model of Alzheimer's disease. *Wellcome Open Research* **2**, 84 (2018).

42. Zaccolo, M., Zerio, A. & Lobo, M. J. Subcellular Organization of the cAMP Signaling Pathway. *Pharmacological Reviews* **73**, 278–309 (2021).

43. McPhee, I. *et al.* Cyclic nucleotide signalling: a molecular approach to drug discovery for Alzheimer's disease. *Biochemical Society Transactions* **33**, 1330 (2005).

44. Sassone-Corsi, P. The Cyclic AMP Pathway. *Cold Spring Harbor Perspectives in Biology* **4**, a011148–a011148 (2012).

45. Naqvi, S., Martin, K. J. & Arthur, J. S. C. CREB phosphorylation at Ser133 regulates transcription via distinct mechanisms downstream of cAMP and MAPK signalling. *Biochemical Journal* **458**, 469–479 (2014).

46. Mussbacher, M. *et al.* Cell Type-Specific Roles of NF-κB Linking Inflammation and Thrombosis. *Frontiers in Immunology* **10**, (2019).

47. Sugawara, K., Shibasaki, T., Takahashi, H. & Seino, S. Structure and functional roles of Epac2 (Rapgef4). *Gene* **575**, 577–583 (2016).

48. Grandoch, M., Roscioni, S. S. & Schmidt, M. The role of Epac proteins, novel cAMP mediators, in the regulation of immune, lung and neuronal function. *British Journal of Pharmacology* **159**, 265–284 (2010).

49. Guo, X.-X. *et al.* Rap-Interacting Proteins are Key Players in the Rap Symphony Orchestra. *Cellular Physiology and Biochemistry* **39**, 137–156 (2016).

50. Renner, M. C. *et al.* Synaptic plasticity through activation of GluA3-containing AMPA-receptors. *Elife* **6**, (2017).

51. Kawasaki, H. *et al.* A Family of cAMP-Binding Proteins That Directly Activate Rap1. *Science (1979)* **282**, 2275–2279 (1998).

52. Bos, J. L. Epac: a new cAMP target and new avenues in cAMP research. *Nature Reviews Molecular Cell Biology* **4**, 733–738 (2003).

53. Schmidt, M., Dekker, F. J. & Maarsingh, H. Exchange Protein Directly Activated by cAMP (epac): A Multidomain cAMP Mediator in the Regulation of Diverse Biological Functions. *Pharmacological Reviews* **65**, 670–709 (2013).

54. Ostroveanu, A., van der Zee, E. A., Eisel, U. L. M., Schmidt, M. & Nijholt, I. M. Exchange protein activated by cyclic AMP 2 (Epac2) plays a specific and time-limited role in memory retrieval. *Hippocampus* **20**, 1018–1026 (2010).

55. Pereyra, M. & Medina, J. H. AMPA Receptors: A Key Piece in the Puzzle of Memory Retrieval. *Frontiers in Human Neuroscience* **15**, (2021).

56. Bast, T. Distinct Contributions of Hippocampal NMDA and AMPA Receptors to Encoding and Retrieval of One-Trial Place Memory. *Journal of Neuroscience* **25**, 5845–5856 (2005).

57. Bliss, T. V. P. & Cooke, S. F. Long-term potentiation and long-term depression: a clinical perspective. *Clinics* **66**, 3–17 (2011).

58. Rossmann, M. *et al.* Subunit-selective N-terminal domain associations organize the formation of AMPA receptor heteromers. *The EMBO Journal* **30**, 959–971 (2011).

59. Lu, W. *et al.* Subunit Composition of Synaptic AMPA Receptors Revealed by a Single-Cell Genetic Approach. *Neuron* **62**, 254–268 (2009).

60. Gasbarri, A. & Pompili, A. Involvement of Glutamate in Learning and Memory. in *Identification of Neural Markers Accompanying Memory* 63–77 (Elsevier, 2014). doi:10.1016/B978-0-12-408139-0.00004-3.

61. Danysz, W. & Parsons, C. G. Alzheimer's disease, β-amyloid, glutamate, NMDA receptors and memantine - searching for the connections. *British Journal of Pharmacology* **167**, 324–352 (2012).

62. Lin, C.-H., Huang, Y.-J., Lin, C.-J., Lane, H.-Y. & Tsai, G. NMDA Neurotransmission Dysfunction in Mild Cognitive Impairment and Alzheimer's Disease. *Current Pharmaceutical Design* **20**, 5169–5179 (2014).

63. Aria, M. M. Calcium imaging and optical electrophysiology. in *Electrophysiology Measurements for Studying Neural Interfaces* 105–141 (Elsevier, 2020). doi:10.1016/B978-0-12-817070-0.00005-1.

64. Wong, T. P. *et al.* Hippocampal long-term depression mediates acute stress-induced spatial memory retrieval impairment. *Proceedings of the National Academy of Sciences* **104**, 11471–11476 (2007).

65. Tamagnini, F. *et al.* Early Impairment of Long-Term Depression in the Perirhinal Cortex of a Mouse Model of Alzheimer's Disease. *Rejuvenation Research* **15**, 231–234 (2012).

66. Prieto, G. A. *et al.* Pharmacological Rescue of Long-Term Potentiation in Alzheimer Diseased Synapses. *The Journal of Neuroscience* **37**, 1197–1212 (2017).

67. Romberg, C. *et al.* Induction and expression of GluA1 (GluR-A)-independent LTP in the hippocampus. *European Journal of Neuroscience* **29**, 1141–1152 (2009).

68. Migues, P. V. *et al.* PKMζ maintains memories by regulating GluR2-dependent AMPA receptor trafficking. *Nature Neuroscience* **13**, 630–634 (2010).

69. Zhang, Y., Guo, O., Huo, Y., Wang, G. & Man, H.-Y. Amyloid-β Induces AMPA Receptor Ubiquitination and Degradation in Primary Neurons and Human Brains of Alzheimer's Disease. *Journal of Alzheimer's Disease* **62**, 1789–1801 (2018).

70. Kessels, H. W. & Malinow, R. Synaptic AMPA Receptor Plasticity and Behavior. *Neuron* **61**, 340–350 (2009).

71. Gelinas, J. N. *et al.* Activation of exchange protein activated by cyclic-AMP enhances long-lasting synaptic potentiation in the hippocampus. *Learning & Memory* **15**, 403–411 (2008).

72. Schwede, F. *et al.* Structure-Guided Design of Selective Epac1 and Epac2 Agonists. *PLOS Biology* **13**, e1002038 (2015).

73. Pirttilä, T., Kim, K. S., Mehta, P. D., Frey, H. & Wisniewski, H. M. Soluble amyloid beta-protein in the cerebrospinal fluid from patients with Alzheimer's disease, vascular dementia and controls. *J Neurol Sci* **127**, 90–5 (1994).

74. Funahashi, S. Working Memory in the Prefrontal Cortex. *Brain Sciences* **7**, 49 (2017).

75. Tuyttens, F. A. M. *et al.* Observer bias in animal behaviour research: can we believe what we score, if we score what we believe? *Animal Behaviour* **90**, 273–280 (2014).

76. Day, S. J. Statistics Notes: Blinding in clinical trials and other studies. *BMJ* **321**, 504–504 (2000).

77. le Merre, P., Ährlund-Richter, S. & Carlén, M. The mouse prefrontal cortex: Unity in diversity. *Neuron* **109**, 1925–1944 (2021).

78. Uylings, H. B. M., Groenewegen, H. J. & Kolb, B. Do rats have a prefrontal cortex? *Behavioural Brain Research* **146**, 3–17 (2003).

79. Bussire, T. *et al.* Stereologic analysis of neurofibrillary tangle formation in prefrontal cortex area 9 in aging and Alzheimer's disease. *Neuroscience* **117**, 577–592 (2003).

80. Ameen-Ali, K. E. *et al.* The Time Course of Recognition Memory Impairment and Glial Pathology in the hAPP-J20 Mouse Model of Alzheimer's Disease. *Journal of Alzheimer's Disease* **68**, 609–624 (2019).

81. Chavant, F. *et al.* Imipramine, in Part through Tumor Necrosis Factor α Inhibition, Prevents Cognitive Decline and β-Amyloid Accumulation in a Mouse Model of Alzheimer's Disease. *Journal of Pharmacology and Experimental Therapeutics* **332**, 505–514 (2010).

82. Palop, J. J. *et al.* Neuronal depletion of calcium-dependent proteins in the dentate gyrus is tightly linked to Alzheimer's disease-related cognitive deficits. *Proceedings of the National Academy of Sciences* **100**, 9572–9577 (2003).

83. Chen, G. *et al.* A learning deficit related to age and β-amyloid plaques in a mouse model of Alzheimer's disease. *Nature* **408**, 975–979 (2000).

84. Fabbro, S., Schaller, K. & Seeds, N. W. Amyloid-beta levels are significantly reduced and spatial memory defects are rescued in a novel neuroserpin-deficient Alzheimer's disease transgenic mouse model. *Journal of Neurochemistry* **118**, 928–938 (2011).

85. McAlpine, F. E. *et al.* Inhibition of soluble TNF signaling in a mouse model of Alzheimer's disease prevents pre-plaque amyloid-associated neuropathology. *Neurobiology of Disease* **34**, 163–177 (2009).

86. Yamamoto, M. *et al.* Interferon-γ and Tumor Necrosis Factor-α Regulate Amyloid-β Plaque Deposition and β-Secretase Expression in Swedish Mutant APP Transgenic Mice. *The American Journal of Pathology* **170**, 680–692 (2007).

87. Jiang, H. *et al.* Genetic deletion of TNFRII gene enhances the Alzheimer-like pathology in an APP transgenic mouse model via reduction of phosphorylated I B . *Human Molecular Genetics* **23**, 4906–4918 (2014).

88. Jordão, J. F. *et al.* Amyloid-β plaque reduction, endogenous antibody delivery and glial activation by brain-targeted, transcranial focused ultrasound. *Experimental Neurology* **248**, 16–29 (2013).

89. Higaki, A. *et al.* Recognition of early stage thigmotaxis in Morris water maze test with convolutional neural network. *PLOS ONE* **13**, e0197003 (2018).

90. Huang, Y., Zhou, W. & Zhang, Y. Bright lighting conditions during testing increase thigmotaxis and impair water maze performance in BALB/c mice. *Behavioural Brain Research* **226**, 26–31 (2012).

91. Andorfer, C. *et al.* Hyperphosphorylation and aggregation of tau in mice expressing normal human tau isoforms. *Journal of Neurochemistry* **86**, 582–590 (2003).

92. Lewis, J. *et al.* Neurofibrillary tangles, amyotrophy and progressive motor disturbance in mice expressing mutant (P301L) tau protein. *Nature Genetics* **25**, 402–405 (2000).

93. Chin, J. Selecting a mouse model of Alzheimer's disease. *Methods Mol Biol* **670**, 169–89 (2011).

94. Jankowsky, J. L. & Zheng, H. Practical considerations for choosing a mouse model of Alzheimer's disease. *Molecular Neurodegeneration* **12**, 89 (2017).

95. Kim, D.-H., Jang, Y.-S., Jeon, W. K. & Han, J.-S. Assessment of Cognitive Phenotyping in Inbred, Genetically Modified Mice, and Transgenic Mouse Models of Alzheimer's Disease. *Experimental Neurobiology* **28**, 146–157 (2019).

96. Dittrich, G. M. & Heineke, J. TNF-α signaling: TACE inhibition to put out the burning heart. *PLOS Biology* **18**, e3001037 (2020).

Appendices

Content

Appendix 1: List of abbreviations

In Table 1 the abbreviations used throughout this thesis are defined.

Table 1 List of abbreviations used in this report

Abbreviation	Definition
6e10	Antibody against amyloid-beta/amyloid precursor protein (gene)
ABC	Avidin-biotin complex
AC	Adenylyl cyclase
AD	Alzheimer's disease
Akt	Protein kinase B; synonym for PKB
ALS	Amyotrophic lateral sclerosis
AMPAR(s)	α-amino-3-hydroxy-5-methyl-4-isoxazolepropionic acid receptor(s)
ANOVA	Analysis of variance
APP	Amyloid precursor protein
Aβ	Amyloid beta; beta-amyloid
BACE(1)	β-site APP-cleaving enzyme (also known as beta-secretase)
BBB	Blood-brain barrier
BDNF	Brain-derived neurotrophic factor
BSA	Bovine serum albumin
CA	Cornu ammonis
CaMK	Calmodulin-dependent kinase
cAMP	Adenosine 3',5'-cyclic monophosphate; or cyclic AMP
cAMP-GEF	Guanine nucleotide exchange factors for Ras-like small GTPases, directly activated by cAMP; synonym for EPAC
CC	Corpus callosum
CD68	Cluster of differentiation 68 (gene)
CDR	Clinical dementia rating
CFC	Contextual fear conditioning
CI-AMPAR(s)	Calcium impermeable α-amino-3-hydroxy-5-methyl-4-isoxazolepropionic acid receptor(s)
CNS	Central nervous system
CP-AMPAR(s)	Calcium permeable α-amino-3-hydroxy-5-methyl-4-isoxazolepropionic acid receptor(s)
CREB	cAMP-response element-binding protein
DAB	Diaminobenzidine
DAMP(s)	Damage-associated molecular pattern(s)
DD	Death domain
DG	Dentate gyrus
DISC	Death-inducing signalling complex

DPX	Dibutyl phthalate polystyrene xylene
EC50	Half maximal effective concentration
ECs	Endocannabinoids
EPAC	Exchange protein directly activated by cAMP; synonym for cAMP-GEF
EPM	Elevated plus maze
ERK	Extracellular-signal-regulated kinase
FADD	Fas-associated protein with death domain
GAP	GTPase-activating proteins
GDP	Guanosine diphosphate
GEF	Guanine (nucleotide) exchange factor
GPCR(s)	G-protein coupled receptor(s)
GTP	Guanosine triphosphate
GvHD	Graft-versus-host disease
IH	Intrahippocampal
IKK	IκBα kinase (complex)
IL	Interleukin
IP	Intraperitoneal
kDa	Kilo Dalton
kihuTNFR2	Human TNFR2 knock-in (mouse model)
LTD	Long-term depression
LTP	Long-term potentiation
MAP(K)	Mitogen-activated protein (kinase)
mGluR	Metabotropic glutamate receptors
mRNA	Messenger ribonucleic acid
MWM	Morris water maze
NDD(s)	Neurodegenerative disease(s)
NE	Northeast
NFT(s)	Neurofibrillary tau tangle(s)
NFκB	Nuclear factor kappa-light-chain-enhancer of activated B cells
NMDAR(s)	N-methyl-D-aspartate receptor(s)
NO	Nitric oxide
NW	Northwest
PAMP(s)	Pathogen-associated molecular pattern(s)
PB	Phosphate buffer
PBS	Phosphate-buffered saline
PD	Parkinson's disease
PFA	Paraformaldehyde
PI	Phosphatidyl inositol
PKA	Protein kinase A
PKMζ	Protein kinase M zeta
PrP	Prion protein
PSEN	Presenilin
rpm	Rotations per minute
RT	Room temperature
S220	Sp-8-BnT-cAMPS
SC	Subcutaneous
SE	Southeast
solTNF	Soluble form of tumour necrosis factor(-alpha)
SPSS	Statistical Package for the Social Sciences
STAR2	Selective mouse TNF-based agonist of TNF receptor 2

SW	Southwest
TACE	TNF-α converting enzyme; synonym for ADAM17: A disintegrin and metalloprotease 17
TBS	Tris-buffered saline
tmTNF	Transmembrane form of tumour necrosis factor(-alpha)
TNC	Tenascin-C
TNF(-α)	Tumour necrosis factor(-alpha)
TNFR	Tumour necrosis factor receptor
TRADD	TNF receptor 1 associated death domain
TRAF	TNF receptor-associated factor
TX100	Triton X 100

Appendix 2: Supplementary data of pilot study of chronic AD mouse model testing S220 effectiveness on memory retrieval using Morris water maze

In Figure 19 the pilot study MWM experiment prior to data displayed in Figure 17 is given. Data was obtained using the following time line: IP injection with S220 compound or PBS on day 1-14, habituation on day 10-14, and MWM from day 15-24.

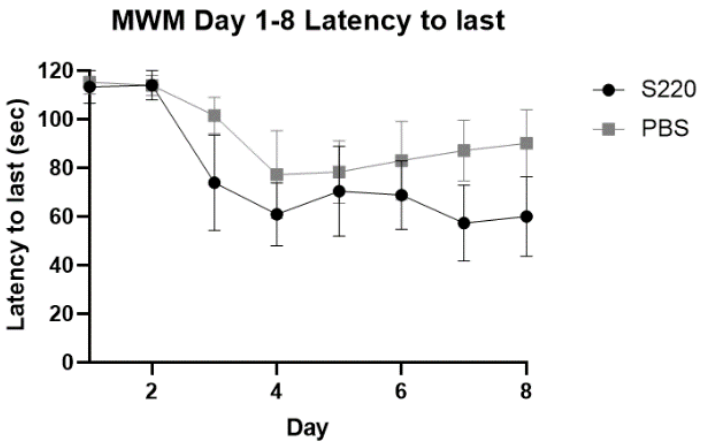

Figure 19 Morris water maze (MWM) training days (day 1-8) shows the S220-treated group (n=4) to find the platform the last time ("Latency to last(sec)", also known as escape latency) generally quicker than the control group (PBS; n=5), though unsignificant. A two-way analysis of variance (ANOVA) repeated measures was performed on the data (p=0.2885). Error bars are standard error of the mean (SEM). Analysis was performed using GraphPad Prism.